NASA CONTRACTOR
REPORT

CR-61119

CR-61119

IMPACT PRESSURE PROBE RESPONSE CHARACTERISTICS IN HIGH SPEED FLOWS, WITH TRANSITION KNUDSEN NUMBERS

Prepared under Contract No. NAS 8-11046 by
J. B. Wainwright and K. W. Rogers

UNIVERSITY OF SOUTHERN CALIFORNIA
ENGINEERING CENTER

For

NASA-GEORGE C. MARSHALL SPACE FLIGHT CENTER
Huntsville, Alabama February 18, 1966

February 18, 1966

CR-61119

IMPACT PRESSURE PROBE RESPONSE CHARACTERISTICS IN HIGH SPEED FLOWS, WITH TRANSITION KNUDSEN NUMBERS
(Date of Report-November 16, 1964)

By

J. B. Wainwright and K. W. Rogers

Prepared under Contract No. NAS 8-11046 by

UNIVERSITY OF SOUTHERN CALIFORNIA
ENGINEERING CENTER

For

NASA-GEORGE C. MARSHALL SPACE FLIGHT CENTER
Huntsville, Alabama

ABSTRACT

N66-20994

Response characteristics of the impact probe in the transitional regime between free-molecule and continuum flows have been investigated both experimentally and theoretically. Experimental data is presented for Knudsen numbers, based on probe diameter, ranging between 0.05 and 10 and with nominal Mach numbers of 1, 3, 6 and 10. The configurations tested were chosen with the view toward separating internal and external probe geometric effects in the transitional regime. Measurements were made with the probes held at the free-stream total temperature and at 41% of total temperature.

The theoretical investigations of probe response were based on a first collision modification of the free-molecule model. Both internal and external effects are calculated and good agreement is shown with the experiments. The free-molecule theory is also extended to the more complicated internal probe geometries which were employed in the experiments.

Application of these investigations to flight measurements is outlined.

Author

TABLE OF CONTENTS

DEFINITION OF SYMBOLS

d	aperture diameter
D	probe diameter
Kn	Knudsen number
ℓ	aperture length
L	tube length
L'	tube length preceeding significant wall collisions
M	Mach number
N	molecular flux/unit area
$N_c(x)$	number of incoming molecules that arrive at station (x) without colliding with the wall
p	probability term
P	pressure
Re	Reynolds number
Re_2	Reynolds number evaluated at conditions behind a normal shock wave
S	speed ratio
T	temperature
P_F	probe pressure under free molecular conditions
P_o'	Rayleigh impact pressure
x	axial coordinate
λ	mean free path
θ	angle of attack
ρ_2/ρ_∞	density ratio across a normal shock wave
ϕ	chamfer angle

DEFINITION OF SYMBOLS (continued) - Subscripts

o	stagnation condition
1	condition at the aperture
F	free molecular flow conditions
D	relative to probe diameter
L	relative to probe length
m	conditions measured at the gauge cavity
T	transitional flow conditions
W	conditions at the wall
x	relative to axial distance
∞	free stream conditions
$\infty - 1$	conditions for the interaction of free stream molecules with aperture molecules
$1-\infty$	conditions for the interaction of aperture molecules with free stream molecules

LIST OF ILLUSTRATIONS

I. INTRODUCTION

The impact pressure probe has long been employed as a primary instrument for the measurement of free stream conditions both in flight and in the wind tunnel laboratory. Its aerodynamic response relative to the free stream is relatively insensitive to geometric configuration and angle of attack and can be readily predicted from inviscid gas dynamics theory. Response in the free molecule flow regime, while sensitive to probe geometry, temperature, Mach number and angle of attack, is still in principle amenable to analysis. In fact, experimental contact with the free-molecule regime is so inaccessible that aerodynamic characteristics in this regime are for the most part only known through analysis.

In contrast, the transitional flow regimes bridging the continuum and free-molecule regimes are not accessible by rigorous analytical techniques, since they ultimately require solutions to the Maxwell-Boltzman equations which treat non-equllibrium distributions of molecular velocities. At the present time, no general solution to these equations has been found which can be applied to the impact probe. There are, however, approximate theories based on simplified models of molecular mechanics which can be applied to the impact probe problem. These combined with appropriate experimental tests promise to provide the basis for extending the usefulness of the impact probe into the transitional regime.

The work described in this report was initiated in July 1963, by the National Aeronautics and Space Administration, Marshall Space Flight Center (Contract number NAS 8-11046) to investigate experimentally and theoretically the response characteristics of impact pressure probes in flows with

transitional Knudsen numbers. These investigations were to be made with the view to applying the impact probe to the calibration of low density supersonic wind tunnel nozzles and to the measurement of atmospheric parameters from high speed flight vehicles.

II. EXPERIMENTS

A. Preliminary Considerations

The response of the impact probe in free-molecule flow is determined by the conservation of mass flux between free stream molecules which enter the probe aperture and the departing molecules which are in thermal equilibrium with the probe cavity. The free-molecule model excludes consideration of collisions among the probe molecules or between probe and free stream molecules. All collisions of significance are between the probe walls and the probe molecules or the free stream molecules.

In considering the initial stages of transition from the free-molecule to continuum response levels it is often useful to employ a "first collision" modification to the free-molecule model in which most of the basic features of free molecule flow are retained, i.e., the juxtaposition of two classes of molecules, free stream and probe, each with Maxwellian distributions and the conservation of mass between free stream molecules entering and probe molecules leaving the probe. The first collision model does, however, consider the effects of single collisions between free stream and probe molecules.

These intermolecular collisions can occur both inside and outside of the probe. The external effects involve scattering of free stream molecules away from the path of the probe aperture by collisions with probe molecules emitted either from the solid front face or from the aperture. This effect, taken alone, reduces the flux of free stream molecules into the aperture and thus reduces the probe cavity pressure relative to the idealized free molecule level. Two competing internal effects can be visualized which foster additional effects. First, in a manner analogous to front face scattering, molecules which would leave the probe are scattered near the threshold of the aperture by collisions with entering free stream molecules. Secondly, collisions between free stream and probe molecules reduce the number of free stream molecules that penetrate to a given station inside of the probe. In effect, the probe molecules offer another mode of wall contact for the free stream molecules so that intermolecular collisions tend to hasten the reduction of the free stream molecular population within the probe relative to the distribution determined by wall collisions alone in idealized free-molecule flow.

These internal effects are of no consequence in the case of the ideal orifice probe where the aperture length is negligible and the dimensions of the cavity are large, relative to the aperture diameter. However, for apertures with finite length-diameter ratios the intermolecular collisions effectively shorten the aperture length, or from another viewpoint, reduce the effective speed ratio of the free stream flow. It will be shown in a later section that the numerical treatments given by de Leeuw and Rothe (1962) and Pond (1962) in extending Clausing's theory of free-molecule flow through tubes to the impact probe, can be modified to approximate the transitional effects of intermolecular collisions.

The impact probe experiments were designed to investigate transitional response characteristics in flow regimes where these first-collision effects could be expected to have application. Both the orifice type and the straight bore, i.e., very large aperture ℓ/d configurations were used. The first enabled a systematic study of variations in internal probe geometry, particularly for small values of aperture ℓ/d. The straight bore configurations provided the limiting opposite extreme for internal geometry relative to the orifice probes and also represented the configuration most frequently used by other investigators. The experiments are described and results discussed relative to the results of first-collision analyses for internal and external effects. The essential features of these analyses are outlined in Section III.

B. Description of Laboratory Facilities

The experiments were divided between the Low Density Wind Tunnel at the University of Southern California Engineering Center and the Hyper-Altitude Simulation Facility of the Naval Missile Center, Point Mugu, California. So far as low density wind tunnel operations are concerned, both facilities are essentially identical. They consist of large cylindrical tanks (10 feet x 20 feet) which are cryopumped using 300 watt gaseous helium refrigerators. These refrigerators in combination with the condensers were capable of continuously pumping at rates of 0.7 gm/sec of nitrogen with intermittent runs as long as a minute for rates as high as 2 gm/sec. Both tanks are fitted with large valves which isolate the condenser from the main chamber in order to permit vacuum breaks

without the necessity of warming up the condenser. These valves also serve as throttles to facilitate the matching of chamber pressure with nozzle exit pressure for specific stagnation conditions and nozzle configurations.

Tests were made in flows from five different nozzles with nominal Mach numbers of 1, 3, 6, 9 and 10. Their general configurations are shown in Figure 1. The Mach 1 nozzle is the Mach 3 nozzle with conical skirt downstream of the throat removed. The Mach 9 nozzle was used only in the USCEC facility and the Mach 10 nozzle only in the Point Mugu facility; the others, Mach numbers 1, 3 and 6, were used in both facilities. With the exception of the Mach 9, the walls of all nozzles were cooled with liquid nitrogen. The test gas for all runs was nitrogen at 300°K. Table 1 gives pertinent dimensions and properties of the nozzles at various stagnation conditions. The methods used for calibration are described in Section II-E where data reduction and correlation procedures for the impact probes are discussed.

C. Description of Probes

The geometry of the basic orifice probe Series A designs is illustrated in Figure 2. The aperture was centered in a thin flat face with diameter equal to 0.2 of the outside diameter and length equal to 0.25 of the aperture diameter. The cavity behind the aperture was 0.8 D and had a length of 10 D. This geometry was applied to a set of 5 probes ranging in diameter from 0.05 inches to 1.0 inches. These were used to calibrate the nozzles and, at the same time to establish the response

characteristics of the design over a factor of 200 range in Knudsen number.

Variations in aperture ℓ/d were investigated with the Series B configurations, in which all geometric features except aperture ℓ/d were fixed on a set of five 0.1 inch diameter probes. ℓ/d ranged between 0.1 and 2. Another 0.1 diameter probe was constructed identical to the $\ell/d = 2$ probe except that its front face was chamfered 45°. The relative outputs of these two probes provided a measure of external free stream scattering effects from the probe face because of their identical internal geometry.

The Series C straight bore probes had an internal ℓ/d of about 40 with outside diameters ranging from 0.032 inches to 0.375 inches.

The Series A and B probes were tested at ambient temperature (about $290^{\circ}K$) and at $125^{\circ}K$. Cooling was accomplished by attaching a liquid nitrogen line to the probe base attachment fitting. (See Figure 3). All of the Series A and B probes, except those of Series A, 0.5 inches and 1.0 inches in diameter, were made of brass. For these the thermal conduction rate from base to tip exceeded the combined radiative and gas conduction losses by a factor of 3 or 4. Temperatures were measured on the $\frac{1}{4}$-inch copper tubing joining the probe to the attachment fixture. The estimated increment in temperature between measurement point and probe tip is less than $5^{\circ}K$. The Series C probes were made of stainless steel and their thermal conduction properties were so poor that no cooling runs were attempted.

D. Description of Apparatus and Instrumentation

A movable probe carriage permitted the consecutive testing of five configurations per run. Each group of five were connected to a common manifold through solenoid operated isolation valves. Manifold pressure was measured with a movable diaphragm differential pressure transducer with a variable capacitance sensor. The nominal range of this instrument was 0-600 microns Hg. It was calibrated with a device which introduces incremental measured quantities of gas into a known test volume. The minimum incremental pressure step used in the calibration was 1 ± 0.1 microns. The transducer produced a linear output within 1% of reading in the range 10-500 μ Hg. The reference side of the transducer was vented to the test chamber. Chamber pressure was measured with a McLeod gauge in the USCEC facility and with a thermocouple pressure transducer in the Point Mugu facility. Both instruments were capable of resolving 0.2 μ in the range 0.5 μ to 20 μ . Reservoir stagnation pressures were measured with the same transducer as the impact probes at Mach numbers 1 and 3 with a variable inclination unity oil manometer at the higher Mach numbers. Accuracy of the latter instrument was within 1% of reading.

In a typical sequence of testing, a given flow condition was established and each probe configuration was positioned in turn at the nozzle centerline and valved into the pressure transducer. Typical response times for the measurement varied from a few seconds to three minutes, depending on pressure level and probe geometry.

E. Data Reduction and Correlation

Measured impact pressures were normalized with the idealized Rayleigh impact pressure derived from nozzle calibrations. Since the variation in nozzle boundary layer thickness, Mach number, Rayleigh pressure, etc., which accompany the variation in reservoir pressure are large in low density nozzles, the nozzle calibration involves the simultaneous calibration of both the nozzle and the probe configuration used in the calibration. It was assumed in the present calibration procedure that the transitional response properties of the geometrically similar probes of Series A, characterized by the ratio of measured pressure to Rayleigh pressure versus Knudsen numbers are not altered for the limited range of Mach numbers produced by a single nozzle. With this assumption the Rayleigh impact pressures associated with the various reservoir stagnation pressures driving the nozzle are simply those which force the correlation of the measurements from all Series A probes and at all reservoir pressures. The data were first normalized with reservoir pressure and plotted at constant reservoir pressure versus a provisional Knudsen number based on trial estimates of Mach number and Reynolds number. With this plot, determinations of Rayleigh reservoir pressure ratios P_o/P_o' were made which correlated all of the constant reservoir pressure data on a single characteristic probe response curve of P_m/P_o' versus Knudsen number. The final Knudsen numbers were based on the Mach numbers and Reynolds numbers corresponding to the derived values of P_o'/P_o. The success of the method is illustrated in Figures 4b, 4c and 4d for the final calibration results of the Mach number 3, 6 and 10 nozzles. In the case of the sonic nozzle the chamber pressure

was adjusted to the sonic exit pressure corresponding to the various reservoir pressure settings and the Mach number was taken as unity. Final values of Mach numbers and Reynolds numbers were derived from the ratio of Rayleigh impact pressure and reservoir pressure.

The 0.9 power law was used for the temperature dependence of viscosity in the Reynolds number determination. Reference conditions were taken at 200°K. This approximation is of simpler form and yields a better fit to experimental viscosity measurements for the temperature ranges considered than does the Sutherland approximation.

Thermal transpiration corrections associated with the $\frac{1}{4}$-inch tubing connecting the probes to the water cooled isolation valves were imposed for the runs with probe cooling using the techniques of Arney and Bailey (1962).

F. Results

1. Series A Probes

With the exception of the case for Mach number 10, the transitional characteristics shown in Figure 4 for the Series A probes were measured over a large enough Knudsen number range to bring the response to within a few percent of the theoretical free-molecule value. In spite of this, the data displays little

tendency of following an asymptotic approach to the free-molecule level as the first collision theory suggests. The theory does, however, predict rather well the over-all extent of the transition interval as evidenced by the slope of the data and theory on the semi-log plot.

As might be expected from the results of other investigators, notably Potter and Bailey (1963), and Matthews (1958), it was found that free stream Knudsen number is not a suitable parameter for correlation of the initial rise of probe response from the continuum level. Potter and Bailey (1963) have shown that the parameter, $Re_2 (\rho_2/\rho_\infty)^{\frac{1}{2}}$, is consistent with the viscous layer and merged layer concepts and have successfully used it to correlate a large body of experimental data in these flow regimes. The subscript "2" refers to conditions behind the inviscid normal shock and ρ_2/ρ_∞ is the normal shock density ratio. The reciprocal of the parameter has been used to correlate the Series A probe data for all Mach numbers in Figure 5. This has the effect of shifting the ordinant, relative to free stream Knudsen number, by factors of 0.670, 0.275, 0.322 and 0.420, respectively, for Mach numbers 1, 3, 6 and 10.

The pressure response parameter $(P_n - P_o')/(P_F - P_o')$, that is, the ratio of the difference of measured and Rayleigh impact pressures to the difference of free-molecule and Rayleigh impact pressure, is used in order to normalize the various levels of free-molecule response at different Mach numbers. It is seen that the initial rise relative to these parameters corresponds to values of $Re_2(\rho_2/\rho_\infty)^{-1}$ of 0.05 to 0.10. This is in substantial agreement with the Potter and Bailey (1963) result which shows the rise beginning at 10-20 relative to $Re_2(\rho_2/\rho_\infty)^{\frac{1}{2}}$. Figure 5 also indicates that the correlation extends well beyond the initial rise point

particularly for the lower Mach numbers. With increasing Mach numbers, departure from the line of correlation occurs at correspondingly lower values of $Re_2(\rho_2/\rho_\infty)^{-1}$. This feature is believed to be a consequence of the internal geometry of the Series A probe and will be discussed in Section 3 below.

2. Aperture ℓ/d Effects

The results of the aperture ℓ/d effects measured with the Series B probes are summarized in Figures 6a through 6d. Theoretical values are shown both for the free-molecule limit and for the transitional Knudsen numbers which were tested. In the latter case, collisions between free stream and probe molecules are only accounted for within the length of the aperture and no correction is made for the effects of the distributions of collisions on the tube wall and with molecules aft of the aperture. Rather, the levels for these theoretical values are arbitrarily set at the measured value corresponding to ℓ/d = zero in order to facilitate the comparison of experimental and theoretical ℓ/d effects. The theoretical free-molecule values, however, do account for the collision distribution of free stream molecules with the tube walls and the tube-aperture junction effects for molecules leaving the tube, as well as the aperture ℓ/d effects computed by deLeeuw and Rothe (1962) for the idealized aperture opening into a large cavity.

The most evident features diaplayed by these plots are the persistence of free-molecule pressure rise characteristics into the transitional

regime of Knudsen numbers for small values of ℓ/d and the abrupt departure from this trend between $\ell/d = 1$ and $\ell/d = 2$. The latter feature becomes increasingly pronounced with increasing Mach number. It is attributed to collisions between free-stream and probe molecules within the aperture section and the fact that these collisions have a larger effect at higher Mach numbers because the entering molecular flux is more directed and the probability of free stream collisions with the aperture wall is reduced. In effect, the collisions between free stream and probe molecules within the aperture tend to "cut off" the aperture length.

An additional illustration of this effect is found in Figure 7 where the response characteristics of the straight bore (Series C) probes are presented in the same form used for the Series A probes in Figure 5. It is seen that, as before, the points of initial pressure rise are correlated with the parameter $Re_2(\rho_2/\rho_\infty)^{-1}$. The most notable feature in Figure 7, however, is the variation with Mach number of the interval of Knudsen number required to complete the transition to the free-molecule response levels.

At Mach numbers 1 and 3 it appears that a two order of magnitude change in Knudsen number is sufficient, while at Mach number 10 a four order of magnitude change may be required. This is due to a relatively higher probability for the free stream molecules to penetrate deep into the aperture before striking the wall at the higher Mach numbers. Thus, correspondingly greater reductions in molecular density inside of the probe must be achieved in order to eliminate all but a negligible number of molecular collisions and bring about the free-molecule distribution of collisions between free stream molecules and the interior probe walls and bring about the free-molecule distribution.

The elimination of molecular collisions is further retarded by the fact that the higher Mach numbers produce larger pressure increments relative to the Rayleigh impact pressure for probes with large ℓ/d apertures.

3. Effects of Interior Geometry

It is now convenient to make at least a qualitative comment on the departures of the Mach numbers 6 and 10 data from the Series A probe correlation curves in Figure 5. In free-molecule flow, the tube sections aft of the apertures on the Series A and B probes are in every sense impact tubes with respect to the free stream molecules which have not suffered collisions with the aperture walls. With a procedure analogous to that used to compute the pressure response of impact tubes with finite aperture ℓ/d, the pressure rise associated with the distribution of free stream molecule collisions on the tube walls can be computed provided due account is taken of the effect of the aperture on the end when considering the flux of molecules out of the tube. The differences between the response of the Series A probes (with aperture $\ell/d = 0.25$) and the idealized infinite cavity case, with the same aperture ℓ/d, is only a few percent at Mach numbers 1 and 3; but it rises to 13% at Mach number 6 and to 27% at Mach number 10. This larger contribution from the tube section at higher Mach numbers is attributed to the larger fraction of free stream molecules that get through the aperture and the high probability that these will travel far into the tube before colliding with the wall.

The transition effects associated with tube section at Mach numbers 1 and 3 are negligible since the total free molecule effect is only 3%. However, for the higher Mach numbers, full transition to the free molecule response will not be realized until all but a negligible fraction of the molecular collisions within the tube section are eliminated. Thus, in Figure 5 the long ℓ/d transition characteristics associated with the tube section, and similar to the straight bore probe characteristics, are seen to emerge from the line correlating what are essentially the aperture transition characteristics.

4. External Collision Effects

Collisions between molecules emitted from the front face of an impact probe and free stream molecules in the path of its aperture constitute the remaining source of transitional effects. Theoretical treatments of this problem using first collision considerations have been made by Liu (1958) and more recently by Kinslow and Potter (1963) in connection with the drag of a sphere. Modifications to these analyses are outlined below in Section III.

An experiment designed to secure a measure of these scattering effects was performed by measuring the relative responses of two Series B probes having identical internal geometries, i.e., $D = 0.10$ and $\ell/d = 2.0$, but with differing external geometries. One had the standard flat face of the A and B Series probes while the face of the other was chamfered at 45°.

If it is assumed that reflections from the face are diffuse and the effect of the chamfered face is to dilute the intensity of the effused molecules which can produce scattering collisions by the ratio of the projected frontal area to the actual area of the chamfered face, then the ratio of scattering intensity from the chamfered face to that for that of the flat face is $\cos\phi$, where ϕ is the chamfer angle.

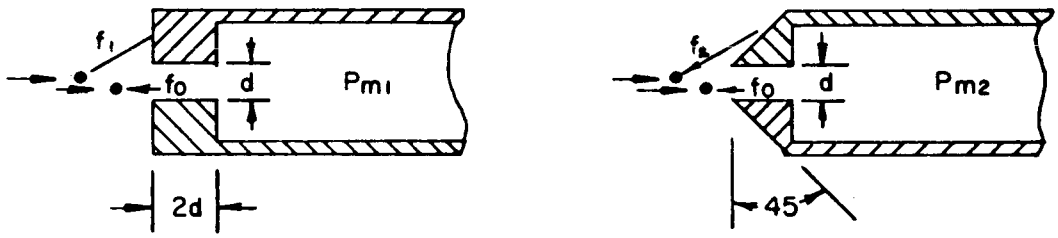

Now referring to the figure, let

f_1 = the scattering fraction associated with the flat face

f_2 = the scattering fraction associated with the chamfered face

f_o = the scattering fraction associated with the aperture

P_{m_1} = measured impact pressure for flat faced probe

P_{m_2} = measured impact pressure for chamfered faced probe

then

$$f_2 = f_1 \cos\phi$$

and

$$\frac{P_{m2}}{P_{m1}} = (1-f_o - f_1 \cos\phi) \Big/ (1 - f_o - f_1) \qquad (1)$$

Solving for f_1

$$f_1 = (1-f_o)\,(P_{m2}/P_{m1} - 1) \Big/ (P_{m2}/P_{m1} - \cos\phi) \qquad (2)$$

If the aperture to face area ratio is small, as it is for the Series B configurations, then $f_o \ll 1$ and noting $N_1/N = 1 - f_1$

$$N_1/N_\infty = 1 - (P_{m_2}/P_{m_1} - 1)(P_{m_2}/P_{m_1} - \cos\phi) \tag{3}$$

The measurements from the chamfered and flat faced probes, expressed in the form of Eq. (3), are presented in Figure 8 and compared with the scattering theory. It is seen that the measurements tend to favor Liu's (1958) analysis and give evidence of less scattering than that predicted by the theory outlined in the present paper. The level off and subsequent rise of the measurements at low Knudsen numbers reflects the limit of the free-molecule, "first collision" interpretation of the data and, no doubt, also indicates the limit to which the theory is applicable.

5. Probe Cooling Effects

Figures 4a and 4b show the response characteristics of the Series A probes with wall temperatures held equal to the free stream total temperature and to 0.41 of total temperature. The most notable difference between the two cases is the tendency of the cooled probes pressures to initially fall below both the continuum and free-molecule response levels and then, at the highest Knudsen numbers, to approach the free-molecule level. This non-monotonic behavior is clearly evident at Mach numbers 3 and 6 and is

implied at Mach number 10 where Knudsen number was presumedly not high enough to reverse the downward trend in pressure response.

While there was not sufficient opportunity under the present contract to pursue these cooling effects with detailed analysis or with additional experiments, it appears probable that the observed behavior results from the competition between external and internal transitional effects. There can be no doubt that internal effects are involved throughout the transition interval starting at Knudsen numbers = 0.2. Figures 9a, 9b and 9c show the response of the Series B probes when cooled to temperature ratio $T_w/T_o = 0.41$. The external geometry and size of all of the Series B probes are identical and so should have identical external effects. The differences shown in Figure 9 are, then, due entirely to the effects of aperture ℓ/d. The $\ell/d = 0.1$ and 0.5 cases exhibit the same behavior as the Series A probes (with $\ell/d = 0.25$) and even the $\ell/d = 1$ and $\ell/d = 2$ cases show a delay in the beginning of the transitional pressure rise when compared with the uncooled cases shown in Figure 6.

Additional experiments, designed to determine more extensively the external effects of transition and the effects of cooling on both internal and external effect, will have to be performed in order to gain a clearer picture of the relative importance of these effects. For example, the chamfered probe data, as shown in Figure 8, could be extended to higher and lower Knudsen numbers by testing smaller and larger geometrically similar probes, and the pertinence of the interpretation placed on the data could be assessed with the testing of other chamfer angles. In addition, other probe temperatures should be investigated with the view to more closely simulating actual flight conditions at various Mach numbers.

III. THEORETICAL ANALYSIS

A. Modification of Free Molecular Flow Limit for Series A Probes

In free molecular flow the pressure measured by a gauge depends upon the geometry of the tubing connecting the gauge to the aperture of the probe. Pond (1962) and deLeeuw and Rothe (1962) have made calculations of the free molecular response of gauges mounted on straight bore tubes. These analyses are also appropriate for orifice type probes that are connected to the gauge cavity by large diameter tubing such that the orifice diameter is negligible by comparison. In this section consideration will be given to the change in cavity pressure caused by the use of a finite orifice to tube diameter ratios.

Using the geometry shown in Figure 2, the probe consists of an aperture section of diameter d and length ℓ connected to the gauge cavity by a tube of diameter D and length L. The pressure at the gauge cavity will be assumed to result from a pressure rise across the aperture section and a pressure rise across the tube section. The pressure rise across the aperture section will be that given by the results of deLeeuw and Rothe (1962) for a probe with geometry ℓ/d if a correction is made for any non-Maxwellian distribution of the flow returning into the aperture section. The non-Maxwellian distribution that is significant at a change in tube cross-section results from the gas flowing in the tube. In vacuum technology it is commonly referred to as "beaming." The primary pressure rise in the connecting tube results from those molecules that passed through the aperture section without wall collisions. A

secondary pressure change would result from the non-Maxwellian distribution of the molecules that enter the tube section after striking the wall in the aperture section. This secondary pressure change is small and will be neglected. If the molecules that pass through the aperture section without a collision enter the tube section with the same velocity distribution as those entering the aperture, the pressure rise across the tube section could be related to the results of deLeeuw and Rothe for a probe with geometry L/D . Any change in velocity distribution would be manifested by a change in the distribution of collisions on the wall of the probe. When a comparison is made of the distribution of wall collisions between molecules entering an open tube, and molecules entering the same tube when equipped with a small aperture of negligible length, it is found that while the distribution is altered, the primary effect of the aperture is to shift the starting point for the distribution. Assuming the shift is the only significant change in the distribution, and denoting the starting point by L' , the pressure rise across the section of the tube between the starting point and the gauge cavity can be related to the pressure of a straight bore tube with geometry $(L - L')/D$.

$$\frac{\Delta P}{P_I} = \frac{N_C(\ell)}{N} \left(\frac{d}{D}\right)^2 \left(\frac{P_F}{P_I}\right)_{\frac{L-L'}{D}} \tag{4}$$

$\frac{N_C(\ell)}{N_I}$ = fraction of the incoming molecules that arrive at without colliding with the aperture wall

$\left(\frac{P_F}{P_I}\right)_{\frac{L-L'}{D}}$ = pressure in a straight bore tube with geometry $(L - L')/D$

P_1 = reference pressure equal to the pressure measured behind an infinitely thin orifice in a cavity at the same temperature as the probe

The assumptions leading to Eq. (4) were based on the comparison involving a thin aperture. It is not obvious that a similar velocity distribution would exist if the aperture had a finite length. In the event the distribution is changed by the finite aperture length, the degree of change will increase as the fraction of incoming molecules that pass through the aperture decreases. Since fewer molecules will be involved in any altered distribution, the effects of the alteration will be lessened. For the present analysis any effects will be ignored.

The pressure rise across the length L' can be obtained from the "long tube" approximation. (See Dushman, 1962, for example).

$$\frac{\Delta P}{P_1} = \frac{N_c(\ell)}{N_1} \left(\frac{d}{D}\right)^2 \frac{3}{4} \frac{L'}{D} \tag{5}$$

The gauge pressure can now be approximated by

$$\frac{P_F}{P_1} = \left(\frac{P_F}{P_1}\right)_{\frac{\ell}{d}} + \frac{N_c(\ell)}{N_1} \left(\frac{d}{D}\right)^2 \left[\left(\frac{P_F}{P_1}\right)_{\frac{L-L'}{D}} + \frac{3}{4} \frac{L'}{D} - 1\right] \tag{6}$$

The last term in this expression is a semi-empirical correction to account

for the fact that the pressure drop through a series of components is less than the sum of the pressure drops through the individual units. This is caused by molecular "beaming" in the tube that results in a non-Maxwellian velocity distribution at the junction of the components.

B. External Transitional Effects

When the stream density increases, molecules rebounding from the probe face will travel ahead of the probe and collide with free stream molecules. Some of these collisions will involve free stream molecules that were proceeding into the aperture and, as a consequence of the collision, these incoming molecules will be diverted or scattered from the path of the aperture. While other free stream molecules may be diverted into the aperture, the probability of this occurring is small due to the small solid angle swept out by the aperture.

Liu (1958) and Kinslow and Potter (1963) have investigated the scattering of free stream molecules by molecules rebounding from a probe face and a sphere, respectively. While the calculation details differ, the basic assumption in both analyses is that any collision between a molecule leaving the body and a free stream molecule located in the collision zone prevents that molecule from striking the body. The collision zone is defined as the cylinder extending forward from the body with a cross-sectional area equal to the projected area of the body.

Using this basic assumption, and denoting the fraction of the rebounding molecules that collide with free stream molecules in the collision

zone by $N_{1-\infty}/N_1$, it is found that the rate at which molecules strike a unit area on the body is given by

$$N_1 = N_\infty - N_1\left(\frac{N_{1-\infty}}{N_1}\right) \tag{7}$$

or

$$\frac{N_1}{N_\infty} = \frac{1}{1+\frac{N_{1-\infty}}{N_1}} \tag{8}$$

The results of calculations of this term using the two basic approaches are presented in Figure 10. Also included are the results of a more exact numerical analysis for the same term where $N_{1-\infty}/N_1$ was calculated as the fraction of the rebounding molecules that collided with free stream molecules before passing through the surface of the collision zone.

The results of the analysis which was similar to that by Kinslow and Potter (1963) show the most collisions since that approach applies the maximum collision frequency, i.e., the centerline value, over the entire cross-section of the collision zone. The results of Liu (1958) show the least collisions, since the approximation used overestimates the radial expansion of the rebounding molecules near the probe face.

C. Internal Transitional Effects

1. Introduction

As was outlined in the preliminary discussion of Section II,

intermolecular collisions within the probe have two important effects. One effect is the tendency of the incoming molecules to hinder probe molecules from leaving the exit. Since the investigation of this phenomenon will be limited to collisions with outgoing molecules that would not normally collide with either the wall or another probe molecule before leaving the probe, the effects of this process will be dominated by collisions near the aperture.

The second effect results from the collisions causing the incoming molecules to lose most of their directed character before they strike the wall. This has a similar effect to moving the distribution of wall collisions forward and tends to reduce the gauge cavity pressure. The effects of this process are significant all along the walls of the probe.

2. Internal Scattering

In order to determine the number of probe molecules that are prevented from going out the aperture by collisions with incoming molecules it will be necessary to: (1) determine the distribution of collisions between incoming molecules and probe molecules; (2) determine the number of these probe molecules that were directed towards the aperture; and (3) determine the number of these aperture-bound molecules that would have proceeded to the aperture without colliding with a probe molecule.

In order to estimate the collision rate between incoming and probe molecules, it is necessary to consider the decrease in incoming molecules due to collisions with the wall. It is convenient to use an analytical

approximation for the free molecular flux of incoming molecules that have not struck the wall at a station x. In this approximation, it is assumed that the velocity distribution of the incoming molecules that have not struck the wall is unchanged along the length of the tube. In this case the fraction of the incoming molecules that have not struck the wall becomes

$$\frac{N_c(x)}{N_1} = \exp - \frac{x\Gamma}{D}$$

$$\Gamma = \frac{2\left[1 + \operatorname{erf}(S)\right]}{\exp - S^2 + \sqrt{\pi}\, S \left[1 + \operatorname{erf}(S)\right]} \tag{9}$$

$$\operatorname{erf}(x) = \frac{2}{\sqrt{\pi}} \int_0^x \exp - y^2 \, dy$$

If the radial travel of the molecules is ignored in the calculation of the distance traveled, the collision rate between incoming molecules and probe molecules is obtained by multiplying Eq. (9) by $\exp - (x/\lambda_{\infty - 1}) \frac{dx}{\lambda_{\infty - 1}}$ where $\lambda_{\infty - 1}$ is the mean free path between incoming molecules and probe molecules relative to the probe and must be considered as an average value since the density changes with axial location in the probe.

Of these collisions, approximately one-half were with probe molecules that were moving toward the aperture end of the probe. The fraction of these molecules that were directed toward the aperture can be obtained from free molecular flow concepts. Assuming that the centerline conditions are representative of the cross-section, the fraction oriented toward the orifice is given by $1/\left[1 + (2x/D)^2\right]$.

The fraction of these probe molecules that would have proceeded to the orifice without further collisions with other probe molecules is $\exp(-x/\lambda_1)$ where λ_1 is the mean free path of the probe molecules. If all of these modifications are applied to Eq. (9) and the result integrated over the collision length there is obtained

$$N_{\infty-1} = -N_1 \frac{D}{\lambda_{\infty-1}} \int_0^{L/D} \frac{\exp-\left[\frac{x}{D}\left(\frac{D}{\lambda_{\infty-1}} + \Gamma + \frac{D}{\lambda_1}\right)\right]}{1 + \left(\frac{2x}{D}\right)^2} d\left(\frac{x}{D}\right) \quad (10)$$

$N_{\infty-1}$ = rate of collisions per unit area of entering molecules with probe molecules that (1) were directed toward the aperture, and (2) would not have collided with other probe molecules before reaching the aperture

The upper limit on this expression will vary with the probe geometry since it should include the length of the orifice and some characteristic distance into the cavity to account for internal scattering in this region. Since this integral must be evaluated by approximate methods, and since it is found that the pressure correction resulting from this term is small, the integral has been evaluated with an upper limit of infinity. This produces an error of less than 15% in the correction term if the appropriate distance is greater than a mean free path. This result is included in Figure 10.

3. Modification of ℓ/d Effect Due to Internal Collisions

When incoming molecules strike probe molecules, the incoming molecules are diverted from their original trajectory. Due to the directed nature of the incoming molecules, there is a tendency for these collisions to result in both molecules having an axial motion toward the gauge cavity, but in addition the collisions usually result in both molecules receiving a radial component of velocity. This radial component will generally cause both molecules to contact the wall before moving any significant axial distance. As a result of this wall collision, it is assumed that both molecules lose any directional characteristics and leave the wall with the random distribution. Since the intermolecular collisions occur before the incoming molecules arrive at the axial location of the wall collision in free molecular flow, the principal effect of these intermolecular collisions is to cause the incoming molecules to lose their directed character nearer the aperture than they would in the free molecular flow case. In order to evaluate the effect of these collisions it will be assumed that an incoming molecule loses its directed velocity upon its first collision with either a probe molecule or the wall. This corresponds to the condition of negligible axial movement by the incoming molecule between the intermolecular collision and the next wall collision.

Since this assumption has the effect of altering the distribution of the initial collisions of incoming molecules with the wall, it is necessary to determine the effect of this altered distribution on the gauge pressure. The analysis of this effect will be limited to straight bore probes.

Both Pond (1962) and deLeeuw and Rothe(1962) used the basic development of Clausing (1932) to determine the free molecular pressure in a straight bore probe. By using the continuity equation, they show that the pressure can be approximated by

$$\frac{P_m}{P_1} = \frac{N_m}{N_1} \quad \frac{1}{\left(\frac{N_m}{N_1}\right)_{S=0}} \tag{11}$$

$\frac{N_m}{N_1}$ = fraction of incoming molecules that arrive at the gauge cavity

$\left(\frac{N_m}{N_1}\right)_{S=0}$ = $\frac{N_m}{N_1}$ evaluated at $S = 0$, i.e., probability that a random molecule will proceed through the tube before returning to the entrance.

The term N_m/N_1 can be expressed by

$$\frac{N_m}{N_1} = \frac{N_C(\ell)}{N_1} - \int_0^{\ell} p \frac{d \frac{N_C(x)}{N_1}}{dx} dx \tag{12}$$

p = probability that a molecule striking the wall at x will arrive at the gauge cavity before it arrives at the aperture.

Equations (11,12) were derived for free molecular flow, but they will

apply to the transitional flow if the effects of intermolecular collisions are included in the terms.

The term N_c/N_1, which corresponds to those molecules that have not struck the wall, must be modified since in the transitional flow analysis the initial collisions between incoming and probe molecules are to be considered equivalent to wall collisions. If the radial motion of the incoming molecules is neglected, the transitional flow collision term $(N_c/N_1)_T$ becomes

$$\left(\frac{N_c}{N_1}\right)_T = \frac{N_c}{N_1} \exp - \frac{1}{\lambda_{\infty-1}} \quad . \tag{13}$$

This term can be evaluated by using the numerical methods of Pond (1962) and deLeeuw and Rothe (1962) or less accurately by using the approximation presented in Eq. (9).

Another term in Eq. (12) that may vary with the Knudsen number is the probability term p. Some experimental results obtained from the flow of gases in tubes connecting large chambers have been summarized by Dong and Bromley (1961). These results indicate that the probability is essentially unchanged if the Knudsen number is greater than unity. It has been argued that this is the result of two opposing conditions brought about by the intermolecular collisions. These collisions tend to impede the progress of the molecules since the mean free path between collisions is effectively reduced, but at the same time the collisions tend to generate a mass motion in the tube. These tendencies effectively cancel one another until the Knudsen number decreases below unity where the mass motion dominates and slip flow begins.

The pitot probe represents a more unique condition since there is no chance for a mass motion to develop. This is due to the lack of net mass flow at all stations in the tube. Since there is no net mass flow, it would be expected that the effect of intermolecular collisions would be to reduce the probability. Pollard and Present (1948) have shown that for long tubes this reduction is approximately equivalent to increasing the effective tube ℓ/d by

$$\left(\frac{\ell}{d}\right)_{\text{effective}} = \frac{d+\lambda}{d}\,\frac{\ell}{d} \tag{14}$$

Preliminary calculations indicate that this approach tends to overestimate the changes in probability for short tubes. Since it appeared that a much more sophisticated analytical and experimental investigation would be required to resolve this problem, the simplest assumption was made, that the probabilities are unchanged by the intermolecular collisions. Clausing (1932) developed an approximation for the probability term p which has the form

$$p = a + (1 - 2a)\,\frac{x}{\ell} \tag{15}$$

a = function of ℓ/d only (approximately equal to one-half of the Clausing factor for that ℓ/d).

Using Eqs. (13) and (15), Eq. (12) becomes

$$\left(\frac{N_m}{N_I}\right)_T = a\left[1 + \frac{N_C(\ell)}{N_I}\exp\left(-\frac{\ell}{\lambda_{\infty-1}}\right)\right] + \left(\frac{1-2a}{\ell}\right)\int_0^{\ell}\frac{N_C(x)}{N_I}\exp\left(-\frac{x}{\lambda_{\infty-1}}\right)dx \tag{16}$$

If Eq. (16) is used in Eq. (11), the resulting value of gauge pressure must then be corrected for external or internal scattering. Before applying this correction however, it is useful to compare the uncorrected pressures obtained from the numerical approach of deLeeuw and Rothe (1962) with these obtained from the approximation, Eq. (9). This approximation is particularly convenient since a closed solution can be obtained for $(N_m/N_I)_T$.

$$\left(\frac{N_m}{N_I}\right)_T = a\left[1+\exp-\left(\frac{\Gamma\ell}{d}+\frac{1}{\lambda_{\infty-1}}\right)\right] + (1-2a)\,\frac{1-\exp-\dfrac{\Gamma\ell}{d}+\dfrac{\ell}{\lambda_{\infty-1}}}{\dfrac{\Gamma\ell}{d}+\dfrac{\ell}{\lambda_{\infty-1}}} \tag{17}$$

The uncorrected pressures resulting from the use of Eq. (17) or numerical calculations with Eq. (11) are compared at $S = 2.5$ for a range of Knudsen numbers in Figure 11 a. This figure shows that the largest differences occur in the free molecular flow region so this limiting case is compared for various speed ratios in Figure 11 b. In all of these comparisons, the reference term $(N_m/N_I)_{S=0}$ was evaluated from Clausing's results.

Figure 11 b shows that the approximate solution is useful for an increasing range of L/D as the speed ratio is increased, but for typical supersonic conditions the approximation appears adequate for tubes with $L/D < 1$.

In order to calculate P_m/P_{1_F} it is necessary to apply the corrections that have been developed. This is accomplished by the following expression.

$$\frac{P_m}{P_{1_F}} = \frac{N_1}{N_\infty} \quad \frac{N_m}{N_1} \quad \frac{1}{\left(\frac{N_m}{N_1}\right)_{S=0}} + \frac{N_\infty - 1}{N_1} \qquad (18)$$

IV. APPLICATION OF THE IMPACT PROBE TO FLIGHT MEASUREMENTS

A. Introduction

The impact probe is well established as a primary flight instrument in continuum flows. At flight speeds in excess of 1.5 or 2 times the speed of sound, impact pressure has a weak dependence on Mach number and is very nearly equal to ρU^2, the net momentum flux of the free stream gas. Thus, the impact pressure provides a direct measure of the aerodynamic forces imposed on the flight vehicle structure. In addition, if an independent measure of vehicle velocity is available, which is usually the case for rocket boosted vehicles where radar tracking is employed, then the quotient of the impact pressure and the square of the measured velocity gives the local ambient density of the atmosphere.

Since the free molecule response of an impact probe is determined by the relative rates at which molecules can enter and leave the probe aperture, and not by the momentum which they carry, there are some notable differences between the free-molecule and continuum response characteristics. The most obvious of these is a dependence on the first power of free stream velocity, instead the second power, and a dependence on probe temperature. In addition, it will be shown that Mach number (or speed ratio) has a significant effect which is related to internal geometry and, in fact, this interrelated effect of Mach number and internal geometry can be used to obtain direct, independent measure of Mach number.

The continuum and free molecule response levels are the anchor points for the transitional characteristics of the probe which must be drawn primarily from experiments similar to those described in Section III. The procedures and assumptions involved in reducing wind tunnel experimental data to a form which can be applied to the interpretation of flight measurement will be discussed below. Free molecule response will be considered first and expressed in terms of the independent variables which are usually available in flight measurements.

B. Free Molecule Regime

Since no collisions between molecules are allowed, each species of gas may be considered independently and the flux of free-stream molecules

of species "i" through the aperture is:

$$N_{\infty i} = n_i \sqrt{\frac{2kT_\infty}{m}} \quad \frac{\chi(s)}{2\sqrt{\pi}} \quad \omega\left(\frac{\ell}{d}, s, \theta\right)\Big|_i \tag{19}$$

where s is the molecular speed ratio defined by

$$s = \frac{U}{\sqrt{2\frac{k}{m}T_m}} = \sqrt{\gamma/2} \quad \times \text{Mach number}$$

k = Boltzmann constant

m = mass of a molecule

n_∞ = number density of the species in the free stream

T_∞ = temperature of the species in the free stream

$$\chi(s) = \epsilon^{-S^2} + S\sqrt{\pi}\,(1 + \text{erf}\, S)$$

and $w\left(\frac{L}{D}, s, \theta\right)$ is the probability that a free stream molecule, after entering the aperture with length ℓ and angle of attack θ, will reach the probe cavity. A similar expression can be written for the flux of molecules leaving the probe cavity in which case $w\left(\frac{L}{D}, o, o\right)$ is simply the Clausing factor. Equilibrium requires that the two fluxes be equal. Therefore if the subscripts ∞ and m refer to free stream and probe cavity conditions respectively,

$$n_\infty \sqrt{2\frac{k}{m}T_\infty}\ \chi(S)\,\omega\left(\ell/d, S, \theta\right)\Big|_i = n_m \sqrt{2\frac{k}{m}T_m}\ \chi(0)\,\omega\left(\ell/d, 0, \theta\right)\Big|_i \tag{20}$$

Now if T_∞ is expressed in terms of the free stream velocity (U) and speed ratio, the partial pressure response in the probe cavity for species "i" is

$$P_{mc} = n_m k T_m \Big|_i = \frac{\sqrt{\pi}\, \chi(S)}{2\sqrt{\pi}\, S} \frac{W(\ell/d, S, \theta)}{W(\ell/d, 0, \theta)} U\sqrt{kT_m}\; n_\infty \sqrt{m} \Big|_i \qquad (21)$$

If the speed ratio is greater than 2, the function $\frac{\chi(S)}{2\sqrt{\pi}S}$ is within a fraction of a percent of unity. Then, if the ratio of the "W" probability functions are expressed as $W(\frac{\ell}{d}, s, \theta)$ the summation of all partial pressures is

$$P_m = \sum_i P_{mi} = \sqrt{\pi}\; U\sqrt{2kT_m} \sum_i W(\ell/d, S, \theta)\; n_\infty \sqrt{m_i} \qquad (22)$$

In a gas mixture, the heavier molecules have a larger speed ratio and a corresponding larger value for W. Therefore, the impact probe discriminates to favor a larger concentration of heavy molecules in the gauge cavity than in the free stream.

Now if a free stream mean molecular weight is defined:

$$\bar{m}_\infty = \rho_\infty / n_\infty = \sum_i m_i\, n_{\infty i} \Big/ \sum_i n_{\infty i} \qquad (23)$$

and similarly a mean speed ratio among all species $\bar{S} = U/\sqrt{2kT_\infty/\bar{m}}$

then P_m is written in final form

$$P_m = \sqrt{\pi}\sqrt{\frac{2kT_2}{\bar{m}_\infty}}\,\rho_\infty U\, W(\ell/d,\bar{S},\theta)\sum_i \frac{W(\ell/d,S,\theta)}{W(\ell/d,\bar{S},\theta)}\,\frac{n_i}{n_\infty}\sqrt{\frac{m_i}{m_\infty}} \qquad (24)$$

Figure 12 shows a plot of the function W versus the speed ratio for constant values of aperture ℓ/d and for zero angle of attack. It is seen that if the speed ratio associated with the individual species does not vary from the mean by more than 10 or 20%, then the ratio $W(S_i)/W(\bar{S})$ can be expressed in the approximate form

$$W(S_i)/W(\bar{S}) = 1 - B + B\frac{S_i}{\bar{S}} \qquad (25)$$

where $B = \frac{dw}{ds} \times \frac{\bar{s}}{w(\bar{s})}$

Now, noting that $\frac{S_i}{\bar{S}} = \sqrt{\frac{m_i}{\bar{m}_\infty}}$, the expression under the summation can be written

$$\sum_i = \sum_i \frac{n_i}{n_\infty}\sqrt{\frac{m_i}{m_\infty}}\left[(1-B) + B\sqrt{\frac{m_i}{\bar{m}_\infty}}\right]$$

$$= B + (1-B)\sum_i \frac{n_i}{n_\infty}\sqrt{\frac{m_i}{\bar{m}_\infty}} \qquad (26)$$

A preliminary analysis indicates that for all possible combinations of molecular and atomic nitrogen and oxygen in the atmosphere, the summation $\sum \frac{n_i}{n_\infty}\sqrt{\frac{m_i}{\bar{m}_\infty}}$ is within 1 or 2% of unity. Thus, the free stream density is expressed in terms of the measured parameters

$$\rho_\infty = \frac{P_2}{\sqrt{\pi}\sqrt{\frac{2kTm}{\bar{m}_\infty}}\ U\ W(\ell/d, \bar{S}, \theta)} \tag{27}$$

A note of caution, however, is in order regarding the behavior of atomic species. The response relationship which has been derived tacitly assumes the absence of any recombination within the probe aperture or cavity. The validity of this assumption should be critically investigated, particularly with regard to recombination at the probe wall, before free molecule probes of any description are applied to upper atmosphere measurements where significant decomposition exists. Errors as large as 30% can result depending on the extent of recombination.

If an ionization type sensor is used instead of a pressure sensor, the molecular number density in the probe cavity is the quantity which is measured and must be related to free stream conditions. The response relationship is similar to that for the pressure sensor but is modified to account for the variations in ionization gauge response with respect to gas species.

If C_i is the ionization gauge calibration for species "i", the gauge cavity number density response is:

$$C_i n_{mi} = \frac{2\sqrt{\pi}}{\sqrt{\frac{2kTm}{\bar{m}}}} U n_\infty W(\bar{S}) \frac{W(S_i)}{W(\bar{S})} \frac{n_{\infty i}}{n_\infty} \sqrt{\frac{m_i}{\bar{m}_\infty}} C_i \tag{28}$$

The total indicated gauge density relative to the mean molecular weight of the free stream is

$$\bar{m}_\infty \sum_i C_i n_{mi} = \rho_m = \frac{2\sqrt{\pi} U \rho_\infty W(\bar{S})}{\sqrt{\frac{2kTm}{\bar{m}_\infty}}} \sum_i \frac{W(S_i)}{W(\bar{S})} \sqrt{\frac{m_i}{\bar{m}_\infty}} \frac{n_{\infty i}}{n_\infty} C_i \tag{29}$$

Thus ambient density can be written

$$\rho_\infty = \frac{\rho_m}{2\sqrt{\pi} \frac{U}{\sqrt{\frac{2kTm}{\bar{m}_\infty}}} W(\bar{S}) \sum_i \frac{W(S_i)}{W(S)} \sqrt{\frac{m_i}{\bar{m}_\infty}} \frac{n_{\infty i}}{n_\infty} C_i} \tag{30}$$

Here the quantity to be summed is the same as that for pressure response except for the additional gauge calibration factors, C_i . It is not expected that C_i will differ appreciably for the principal species present in the atmosphere, and the value of the summation will be very near unity.

Four notable differences are seen between the free molecule and continuum response characteristics. First, the free molecule response depends on the first power of probe velocity rather than velocity squared; second,

there is a direct dependence on probe temperature and ambient mean molecular weight; third, there is a dependence on probe internal geometry and attitude through the function W ; and, finally, the effects of recombination and other chemical reactions within the probe aperture and cavity must be accounted for.

The W function is a measure of the probability that a directed molecule with speed ratio s will traverse the aperture length ℓ compared with the probability of molecules with a random velocity distribution. When S , and/or ℓ/d are zero, the value of W is unity. At high speed ratios and finite aperture ℓ/d , the free stream molecule can penetrate deep into the aperture before encountering the wall and W becomes greater than 1. Referring again to Figure 12, it is seen that, for large speed ratios, aperture lengths that are just a fraction of the diameter produce significant increases in probe response.

The effect of flight attitude angle (θ) is essentially to move the distribution of first collisions with the wall forward in the aperture. This effectively cuts off the aperture ℓ/d and the value of W is appropriately reduced. Hughes and deLeeuw (1964) calculate a 5% reduction in pressure with $\theta = 10^{\circ}$ for a probe at Mach number 5 with an aperture L/D = 1. The reduction is 15% for $\theta = 20^{\circ}$. Therefore, if free molecule probes with long apertures are flown at high speed ratios the attitude of the probe must be carefully controlled.

The discriminatory characteristics of the impact tube which favor the heavier molecules appear to be of little consequence, provided the mean molecular weight of the free stream is applied to the speed ratio and the gas constant for the probe cavity molecules. The effects of molecular recombination, however, can be a significant source of error if large concentrations of atomic species are involved.

C. Transitional Regime

It was shown in Section II that for probes with short aperture lengths, the parameter $Re_2 (\frac{\rho_2}{\rho_\infty})^{\frac{1}{2}}$ provided good correlation for experimental data between Mach numbers 1 to 10 over the entire range of transition. Since the short aperture geometry also lends itself readily to flight applications because of short response times and relative insensitivity to angle of attack, the interpretive procedure developed below for flight measurements in the transitional flow regimes will be based on response characteristics similar to those measured for the probe Series A configuration. That is, the response parameter $\frac{P_m - P_o'}{P_F - P_o'}$ will monotonically vary from zero to unity in the interval of about a two order of magnitude change in $Re_2(\frac{\rho_2}{\rho_\infty})^{\frac{1}{2}}$ and will be independent of speed ratio and probe temperature. The experimental evidence argues strongly for this assumption in cases where the probe temperature is held equal to the free stream total temperature. However, in cases where the probe temperature is less than steam total temperature, there are equally strong indications of a non-monotonic response characterized by undershooting the free-molecule level. While this latter situation will most assuredly prevail in actual flight measurements where the probe will be held at a fixed temperature compatible with its associated instrumentation, the monotonic response function will be used for purposes of illustration and the changes in the procedure necessary for the accommodation of probe cooling effects will be indicated.

If the response function is represented by "F", then

$$\frac{P_m - P_o'}{P_F - P_o'} = F\left[Re_2\left(\frac{\rho_2}{\rho_\infty}\right)^{1/2}\right]$$

Normalizing all pressures with ρU^2, the momentum flux of the ambient stream and rearranging

$$\frac{P_m}{\rho U^2} = \frac{P_o'}{\rho U^2} + \left[\frac{P_F}{\rho U^2} - \frac{P_o'}{\rho U^2}\right] F \tag{31}$$

The free-molecule response was given in Eq. (27)

$$\frac{P_F}{\rho U^2} = \sqrt{\pi}\sqrt{\frac{2kTm}{U}} \quad W(\ell/d, \bar{S}) = \sqrt{\pi}\ \frac{1}{Sm} \tag{32}$$

where S_m is defined:

$$Sm \equiv \frac{U}{\sqrt{2kTm}}\ \frac{1}{W(\ell/d, \bar{S})} \tag{33}$$

The continuum response, or Rayleigh pressure, is given

$$\frac{P_o'}{\rho U^2} = \left(\frac{\gamma+1}{2}\right)^{\left(\frac{\gamma+1}{\gamma-1}\right)}(\gamma)^{-\frac{\gamma}{\gamma-1}}\left(1 - \frac{\gamma-1}{2\gamma M^2}\right)^{-\frac{1}{\gamma-1}} \tag{34}$$

and for $\gamma = 7/5$ and Mach numbers greater than 1.5 the expression can be simplified to

$$\frac{P_0'}{\rho U^2} = 0.91\left[1 + \frac{1}{2\gamma M^2}\right] = 0.91\left[1 + \frac{1}{4S^2}\right] \tag{35}$$

Therefore the ratio of measured pressure to ρU^2 in the transitional flow regime is given below

$$\frac{P_m}{\rho U^2} = 0.91\left[1 + \frac{1}{4S^2}\right] + \left[\frac{\sqrt{\pi}}{S_m} - 0.91\left(1 + \frac{1}{4S^2}\right)\right] F\left[Re_2\left(\frac{\rho_2}{\rho_\infty}\right)^{1/2}\right] \tag{36}$$

Figure 13 shows typical variations of this ratio for constant values of S_m using the response function $F\left[Re_2(\frac{\rho_2}{\rho_\infty})^{\frac{1}{2}}\right]$, taken from Figure 5 for the probe Series A geometry.

It is now evident that probe cooling effects can be introduced without undue complication if the data are organized in terms of constant values for the parameter S_m, that is T_m/U^2 = constant. This would not be difficult to manage in the wind tunnel because U^2 is nearly equal to the free stream total temperature for Mach numbers greater than 3 or 4. In this case, the function F would depend on S_m as well as $Re_2(\frac{\rho_2}{\rho_\infty})^{\frac{1}{2}}$ and a new set of plots similar to those in Figure 13 would be generated.

The advantage of organizing the data in this form is that the parameter S_m is known directly from the flight measurements.

The other two independent variables, "S" and $Re_2(\frac{\rho_2}{\rho_\infty})^{\frac{1}{2}}$ cannot be known directly and it will be necessary to make provisional estimates from values of density and temperature given in the standard atmosphere tables. Fortunately, $Re_2(\frac{\rho_2}{\rho_\infty})^{\frac{1}{2}} - 1$ is directly proportional to free stream Knudsen number but only weakly dependent on speed ratio and ambient temperature. (See Figure 14). The other speed ratio dependent function $1 + \frac{1}{4s^2}$ is also of little significance for speed ratios greater than 1.5. For example, a 10% error in estimating ambient temperature for the calculation of speed ratio yields errors in $1 + \frac{1}{4s^2}$ of only 1% at speed ratio 1.5 and 0.3% error at speed ratio 3.

Similarly, Figure 12 shows the probability function W used in the evaluation of S_m to be little affected by speed ratio for small aperture ℓ/d and thus again insensitive to the estimate of ambient temperature.

The density is thus determined from measurements of impact pressure and flight velocity, provisional estimates of density and temperature and an iterative procedure using Eq. (36) which will give successively improved calculations of density and the parameter $Re_2\left(\frac{\rho_2}{\rho_\infty}\right)^{\frac{1}{2}}$. Ambient temperature can also be drawn into the iteration by the procedure outlined below.

D. Determination of RT from Density Profile Measurements

If a succession of density measurements are made over ascending or descending trajectories such as is the case for sounding probes and satellite

boosters, the rate of variation of density with altitude gives a measure of atmospheric specific energy, $\frac{K}{m} T = RT$. The relationship is derived from the statement of equilibrium of forces acting on an elemental volume:

$$\frac{dP}{dH} = -\rho g = \frac{d}{dH} \rho RT$$

Rewriting this equation in terms of RT gives the required relationship:

$$RT = -\left[g + \frac{dRT}{dH}\right] \Big/ \frac{d\ln\rho}{dH}$$

Values of RT altitude gradients are used from the standard atmosphere tables for the initial trial calculation and successive improvements are derived from an iterative procedure.

A more direct determination of RT is feasible in the free molecule regime where the interrelationship between the effects of internal geometry and speed ratio can be exploited. Referring again to Figure 13, it is seen that if simultaneous measurements are made with probes which are identical in every respect except for aperture length diameter ratio, then the ratio of their individual response levels is a monotonic function of speed ratio. Thus if the probe velocity is known, values of RT can be computed directly along the trajectory from the measured speed ratio. This method is particularly attractive at altitudes above 90 KM where large temperature gradients

make the RT determination from density profiles, described above, more difficult. It is well to note, however, that the attitude of the probe would have to be carefully controlled to avoid the degrading effects of angle of attack.

V. Concluding Remarks

The investigations which have been described achieved three essential results. First, the experimental response characteristics of several impact probe configurations were determined over nearly the full interval of transition between the free-molecule and continuum flow regimes and over a wide range of Mach numbers. The configurations were designed to distinguish between internal and external transition effects and the results show a profound influence of both Mach number and probe aperture length on the extent of the transition interval. The results also indicate that the transition interval can be minimized to about two orders of magnitude in Knudsen number by employing probes with very short aperture lengths and large cavity dimensions relative to the aperture diameter.

Secondly, a theory based on a "first collision" modification to the free-molecule model was developed which accounted for much of the experimentally observed internal and external probe characteristics. The free-molecule theory was also extended to probe geometries which lack the idealized simple aperture and large cavity configuration previously

treated by other investigators.

Finally, the techniques for applying the impact probe to the calibration of low density wind tunnel nozzles and to flight measurements in the transitional Knudsen number regime were developed and discussed. The former involves a straight forward separation of nozzle viscous effects from probe effects in the transition regime and can be easily accomplished by employing a set of geometrically similar probes which are relatively insensitive to Mach number changes. Probe configurations with short aperture lengths and large cavity diameters meet the latter requirement and the general procedure is illustrated in Section II E.

Application of the impact probe to flight measurements is more tedious and depends upon the other measurements which are available. Section IV treats the case for the determination of atmospheric density when the probe's speed, altitude and temperature are known, together with the measured impact pressure and a predetermined probe calibration.

There are several aspects of the investigation in which the results were indecisive and incomplete. The most notable of these are the extent to which the theory was applied to the experimental data, the experimental effects and theoretical effects of probe cooling, and a decisive experimental demonstration of free-molecule conditions for the probe. It was an unfortunate circumstance of the program that the development of the theory in its final and most promising form came too late to influence the course of the experiments or to permit even the large number of calculations necessary to compare it with all of the measured data. The most intense interest naturally centers around the probe cooling data because of the unexplained undershooting effect and its direct application to flight measurement.

An equally inconclusive state of affairs exists regarding the experimental achievement of free-molecule conditions. In spite of the fact that Knudsen numbers approaching and exceeding ten were achieved with the Series A probes at Mach number 1, 3 and 6, and that the corresponding response levels were within a few percent of theoretical free-molecule values, the experimental data showed little indication of asymptotically approaching the free-molecule level. It would appear that new experiments designed to produce Knudsen numbers of at least 30 will be necessary to complete the transition interval for short aperture probes. Such experiments are feasible in the Point Mugu Hyperaltitude Facility using a larger nozzle and a more efficient diffuser-cryopump configuration.

LIST OF REFERENCES

Arney, G. D., and Bailey, A. B., (1962). AEDC-TDR-62-188.

Clausing, P., (1932). Annalen der Physik 12, 961-989.

deLeeuw, J. M., and Rothe, D. E., (1962). UTIA Report No. 88.

Dong, W., and Bromley, L. A., (1961). Eighth Vacuum Symposium Transactions, 1116-1132.

Dushman, S., (Lafferty, J. M., ed.) (1962). "Scientific Foundation of Vacuum Technique," 87-90. John Wiley and Sons, New York.

Howarth, L., (1948). Proc. Roy. Soc. (London) A 194, 16-42.

Hughes, P. C., and deLeeuw, J. H., (1964). Book of Abstracts, Fourth International Symposium on Rarefied Gas Dynamics.

Kinslow, M., and Potter, J. L., (1963). AIAA J. 1, 2467-2475.

Liu, V. C., (1958). J. Aero/Space Sci. 25, 779-785.

Matthews, M. L., (1958). GALCIT Hypersonic Research Project Memo No. 44.

Pollard, W. C., and Present, R. D., (1948). Phys. Revs. 73, 762-769.

Pond, M. L., (1962). J. Aero/Space Sci. 29, 917-920.

Potter, J. L., and Bailey, A. B., (1965). AEDC-TDR-63-168.

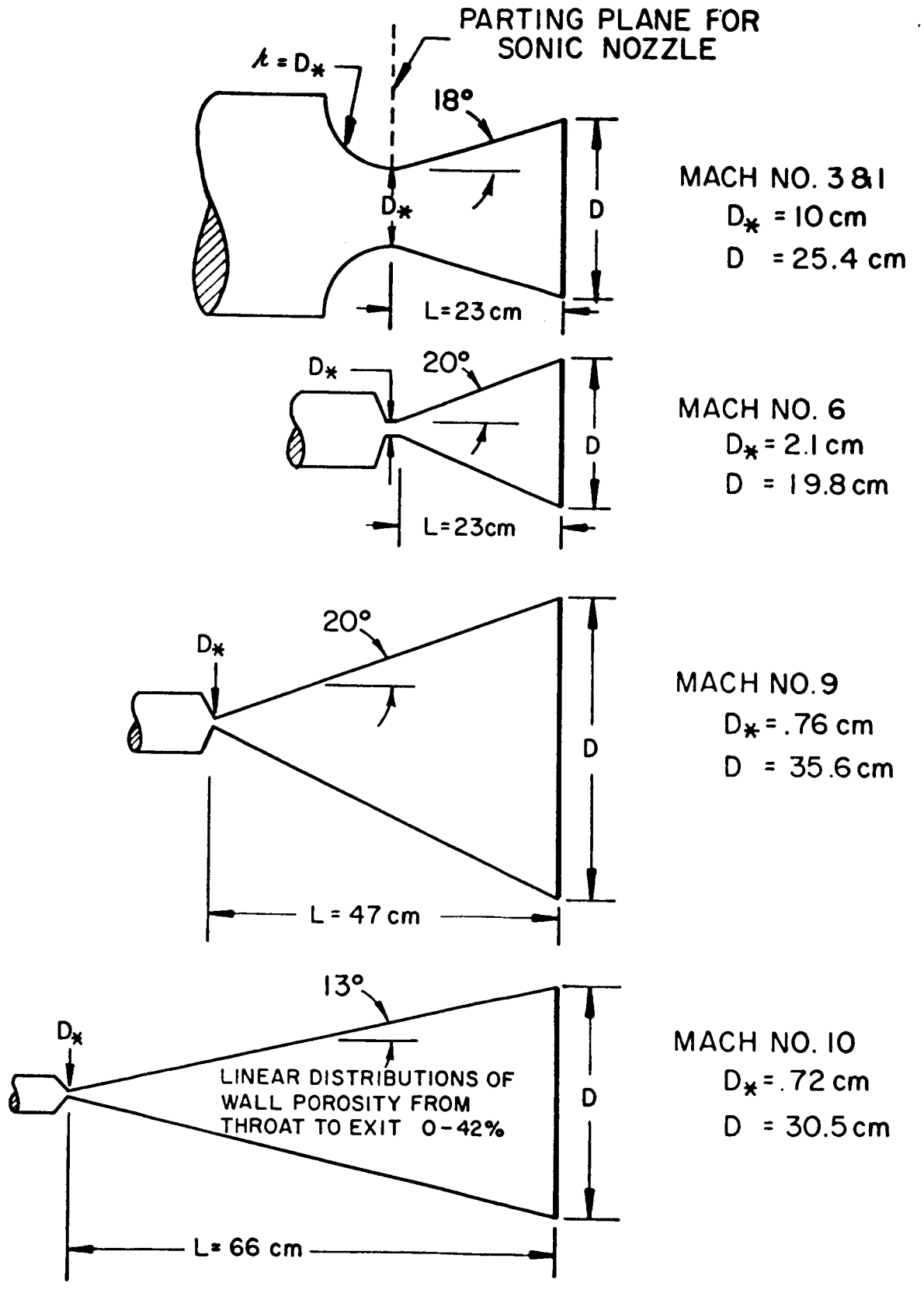

Figure 1. Low Density Nozzle Configurations.

TABLE I

LOW DENSITY NOZZLE PROPERTIES

Nozzle	P_o mm	T_o °K	M	Re/cm	λ_∞ cm	P_∞ μHg	D core cm	ṁ gm/sec
sonic	0.023	290	1.0	4.5	0.33	12.2	1.9	0.06
	0.060			11.7	0.13	31.7	3.5	0.18
	0.108			21.1	0.071	57.0	4.6	0.30
	0.218			42.5	0.035	115	5.8	0.60
	0.400			78.0	0.019	211	7.0	1.1
3	0.020	290	2.90	2.1	2.0	0.63	2.3	0.06
	0.041		3.05	3.9	1.2	1.00	4.8	0.12
	0.061		3.16	5.3	0.89	1.29	6.6	0.18
	0.123		3.29	10	0.49	2.18	9.5	0.37
	0.256		3.38	20	0.25	4.00	12.8	0.67
	0.520		3.47	39	0.13	7.11	15.5	1.46
6	0.51	290	5.53	13.3	0.62	0.53	3.3	0.04
	1.00		5.91	21.6	0.41	0.70	5.5	0.08
	2.00		6.28	37.0	0.25	0.96	7.6	0.19
	4.07		6.58	66.4	0.15	1.46	9.9	0.41
	5.94		6.74	89.0	0.11	1.82	11.2	0.62
	8.11		6.78	120	0.08	2.39	12.2	0.83
	10.14		6.87	147	0.07	2.76	12.7	1.06
9	15.0	290	9.10	96	0.14	0.66	6.1	0.19
	25		9.21	152	0.09	1.02	7.6	0.32
10	14.5	290	9.77	76	0.19	0.40	6.4	0.16
	20.1		10.25	92	0.17	0.40	7.6	0.22
	40.0		10.98	147*	0.11	0.51	8.9	0.44
	59.2		11.38	194	0.09	0.59	9.6	0.65

PROBE	D(INCHES)	d/D	ℓ/D	ϕ
A-1	0.05	0.20	0.25	0
A-2	0.10	0.20	0.25	0
A-3	0.20	0.20	0.25	0
A-4	0.50	0.20	0.25	0
A-5	1.00	0.20	0.25	0
B-1	0.10	0.20	0.1	0
B-2	0.10	0.20	0.5	0
B-3	0.10	0.20	1.0	0
B-4	0.10	0.20	2.0	0
B-5	0.10	0.20	2.0	$\pi/4$

Figure 2. Impact Probe Configurations And Nomenclature.

PROBE	D(INCHES)	d/D	ℓ/D	ϕ
C-1	0.032	0.625	40	0
C-2	0.128	0.780	32	0
C-3	0.128	0.550	45	0
C-4	0.375	0.507	48	0

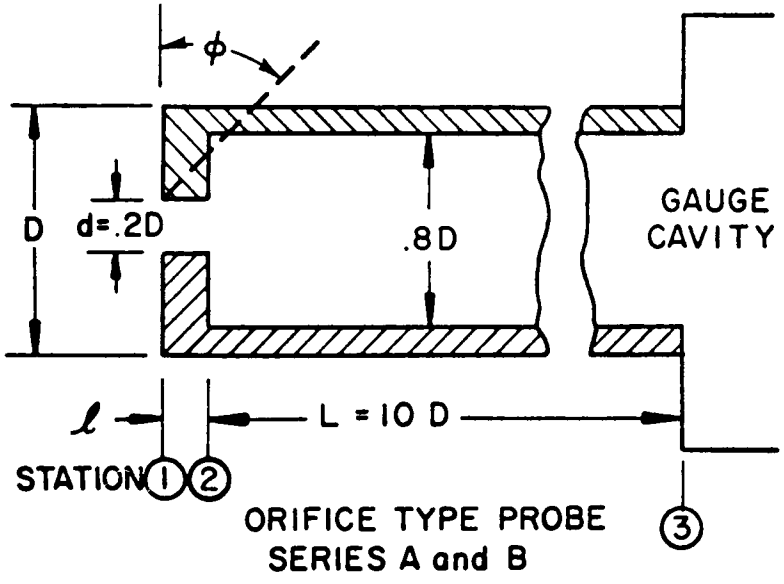

ORIFICE TYPE PROBE
SERIES A and B

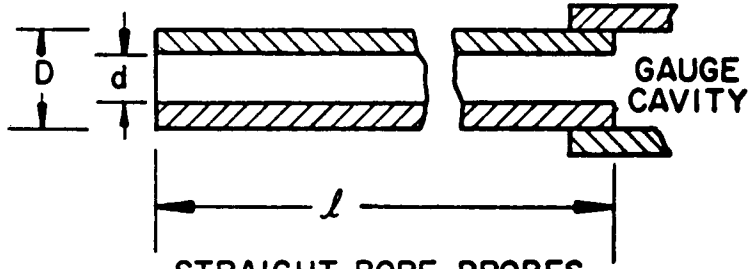

STRAIGHT BORE PROBES
SERIES C

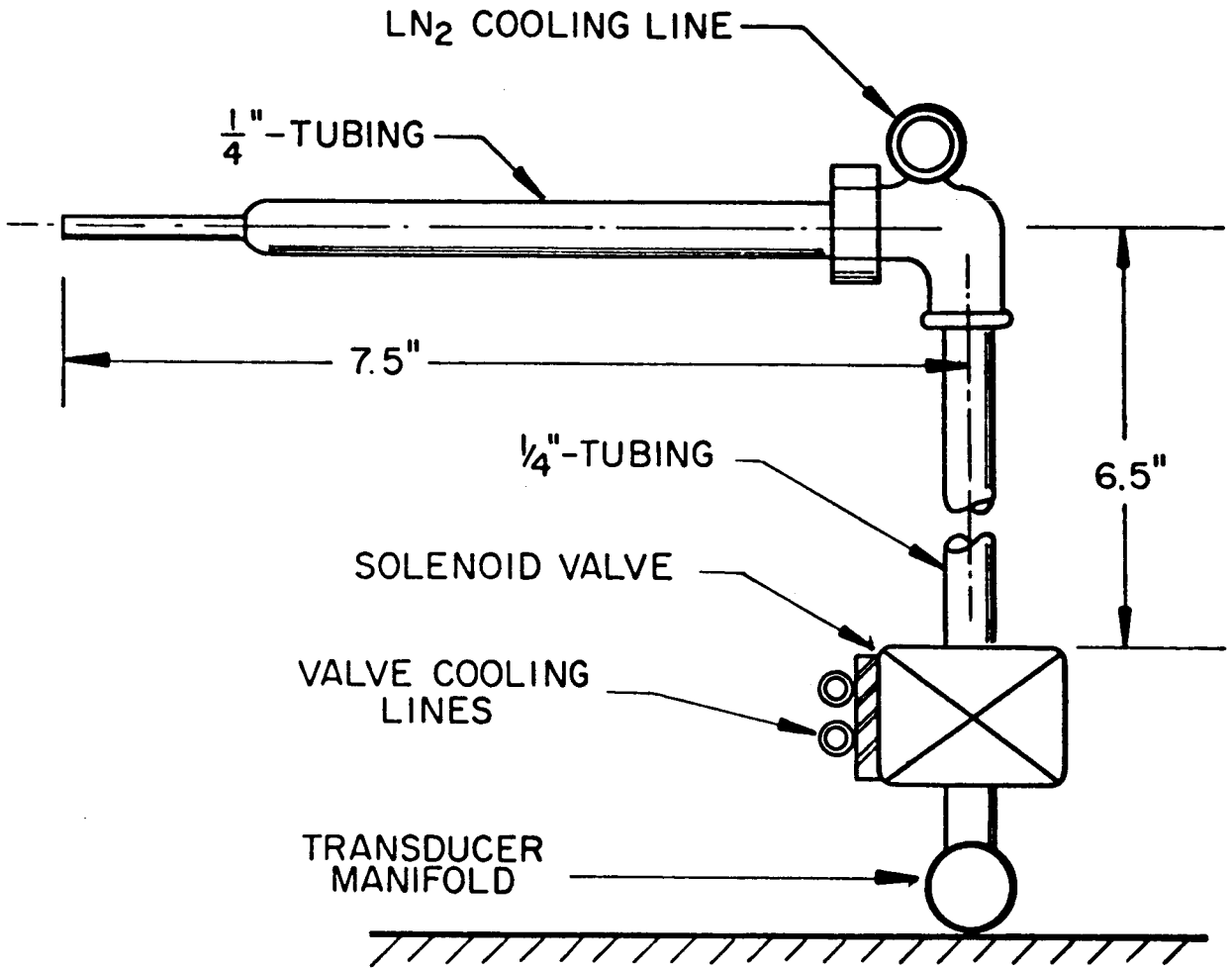

Figure 3. Impact Probes Mounting Arrangement.

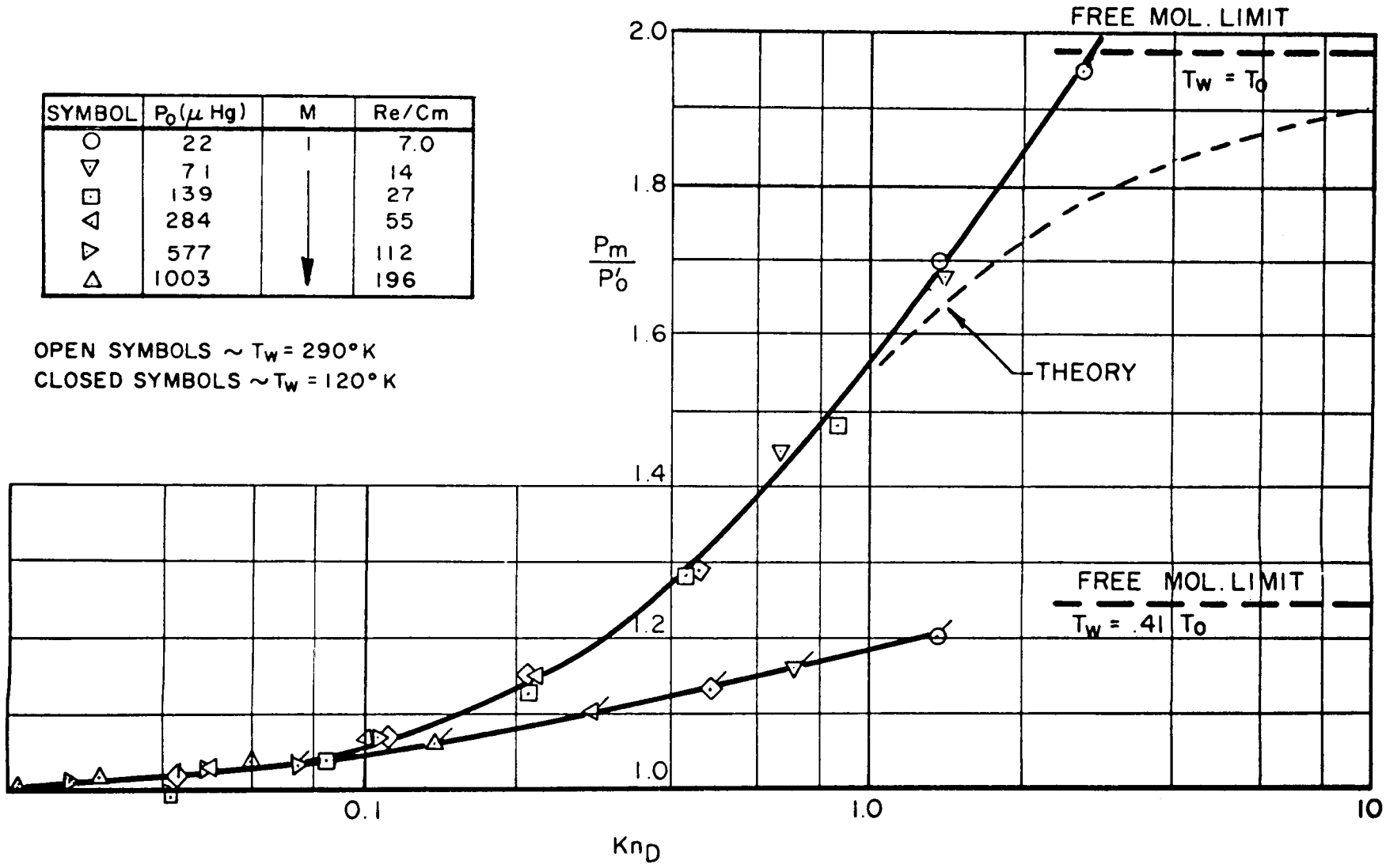

Figure 4a. Series A Impact Probe Response, Mach No. 1

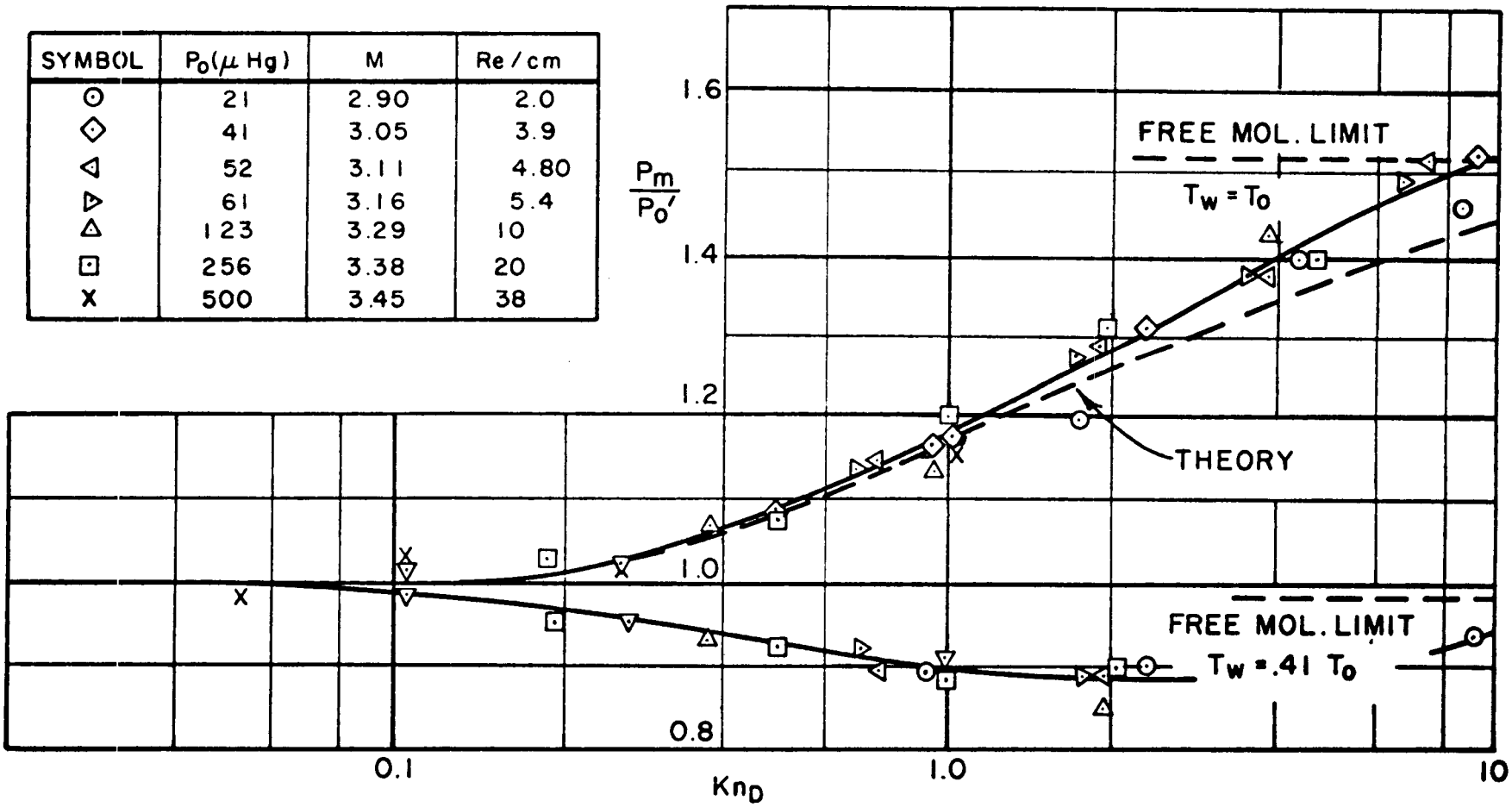

Figure 4b. Series A Impact Probe Response, Mach No. 3.

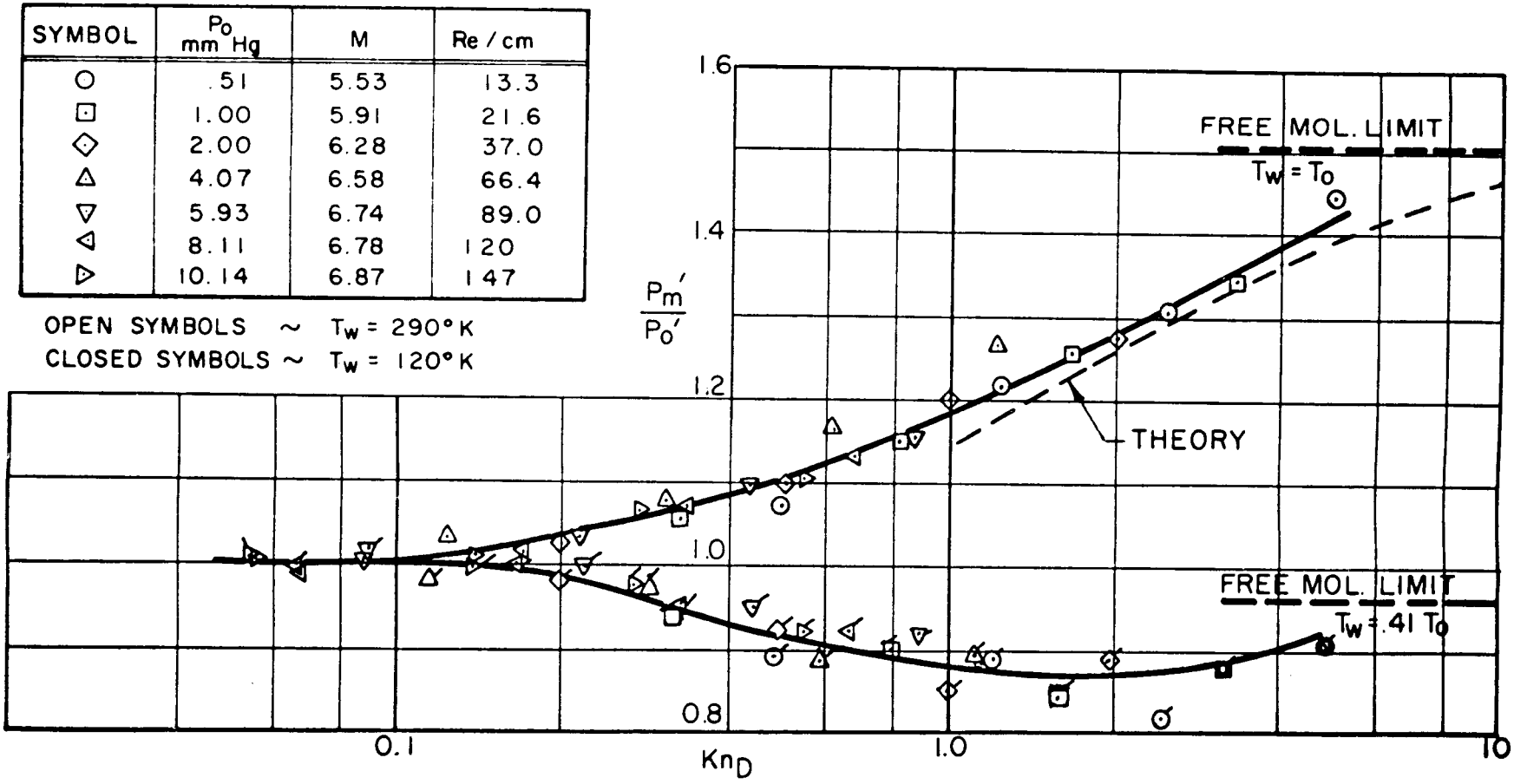

Figure 4c. Series A Impact Probe Response, Mach No. 6.

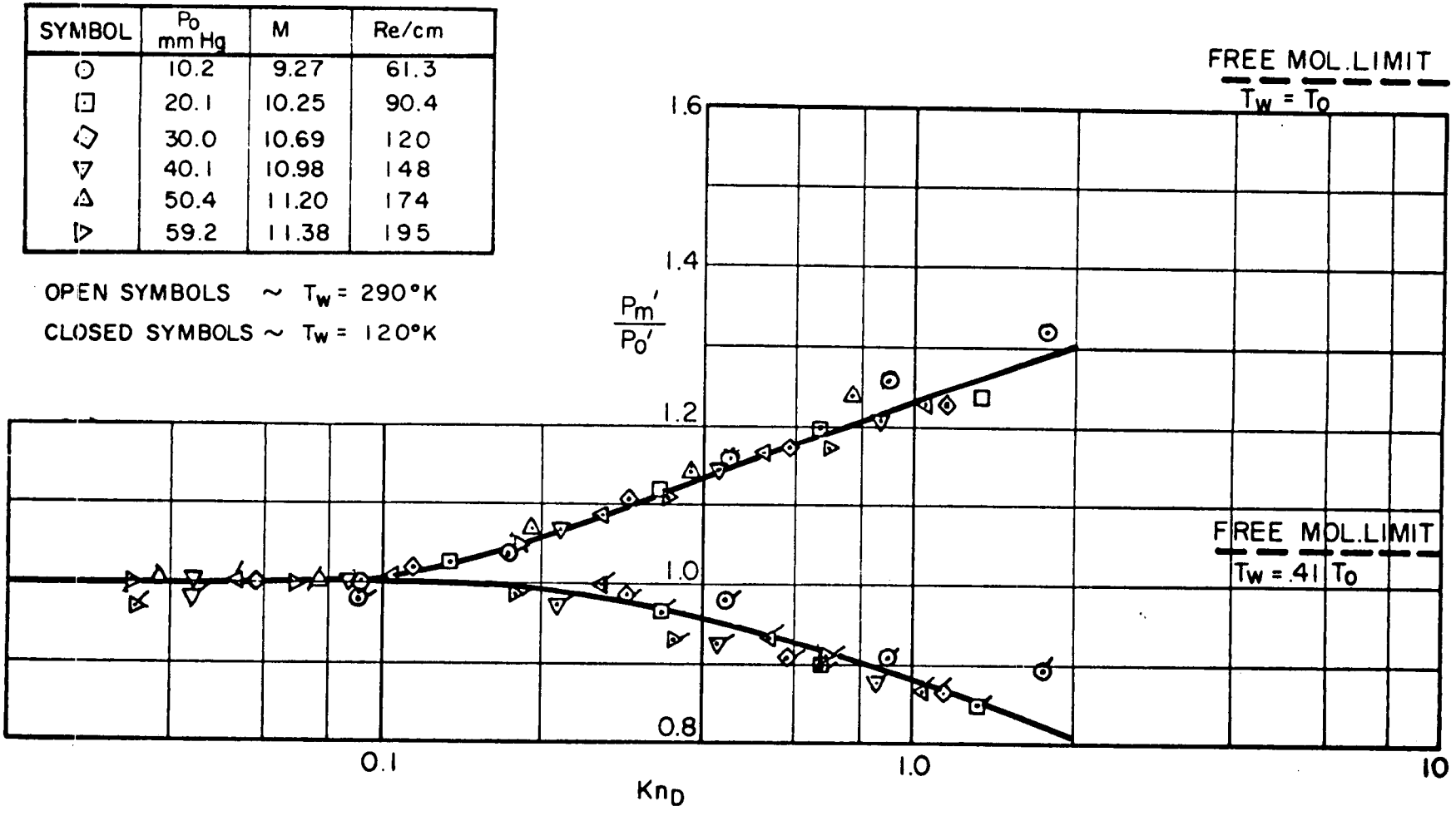

Figure 4d. Series A Impact Probe Response, Mach No. 10.

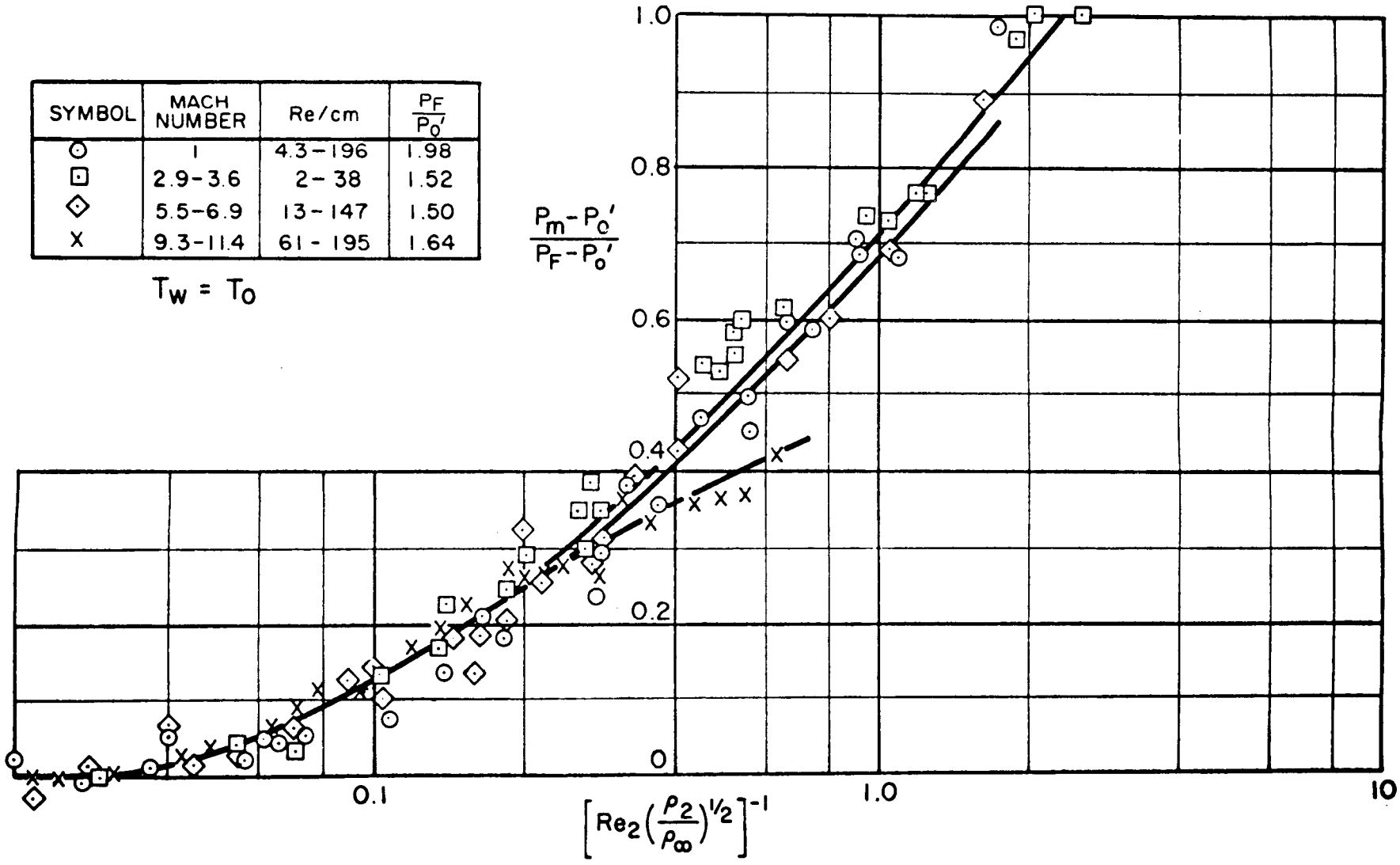

Figure 5. Series A Impact Probe Correlation.

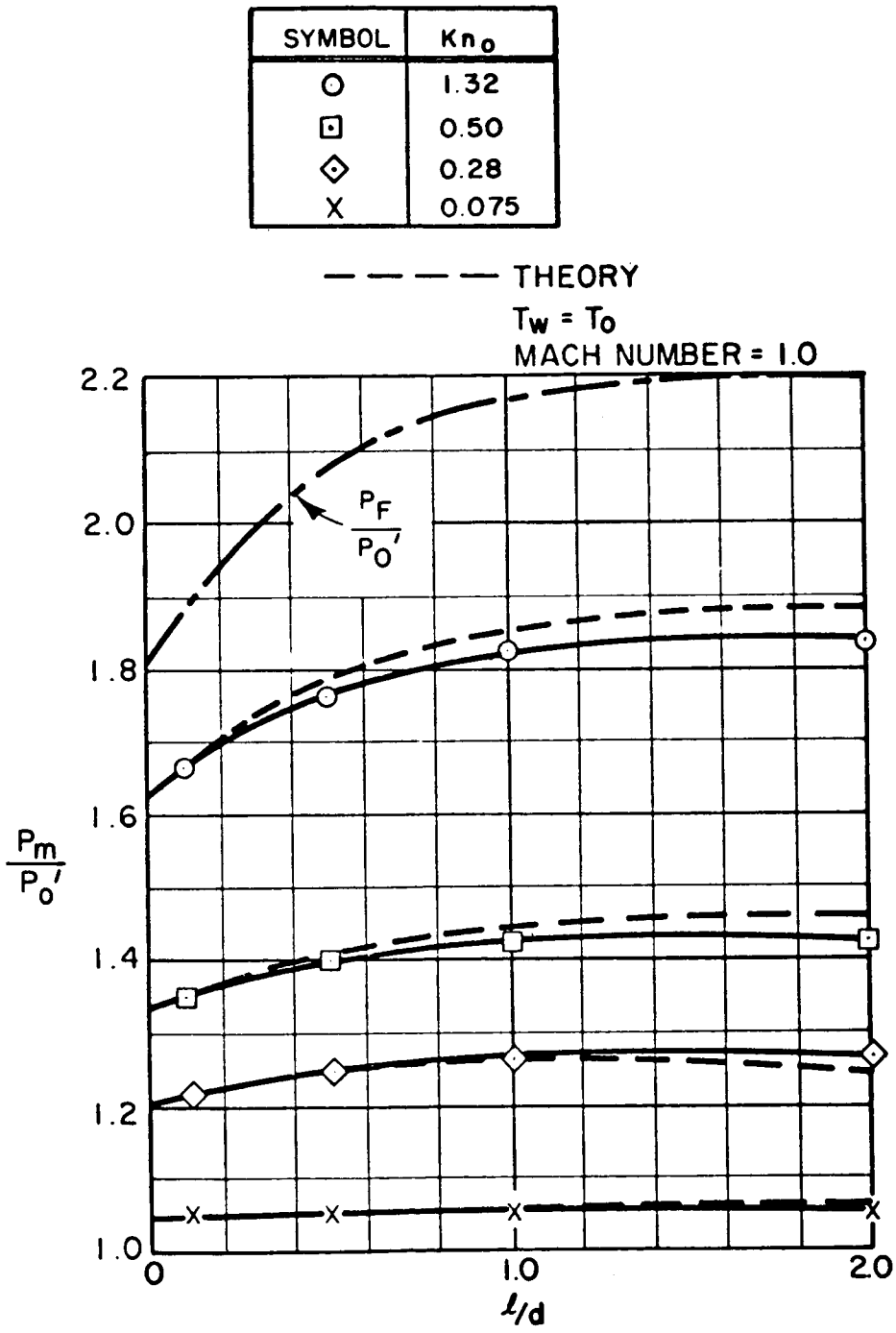

Figure 6a. Series B Impact Probe ℓ/d Effects, Mach No. 1.

SYMBOL	MACH NUMBER	Kn_D
○	2.99	5.9
⊡	3.29	1.9
X	3.38	1.0
◇	3.47	0.52

– – – – – THEORY

$T_w = T_o$

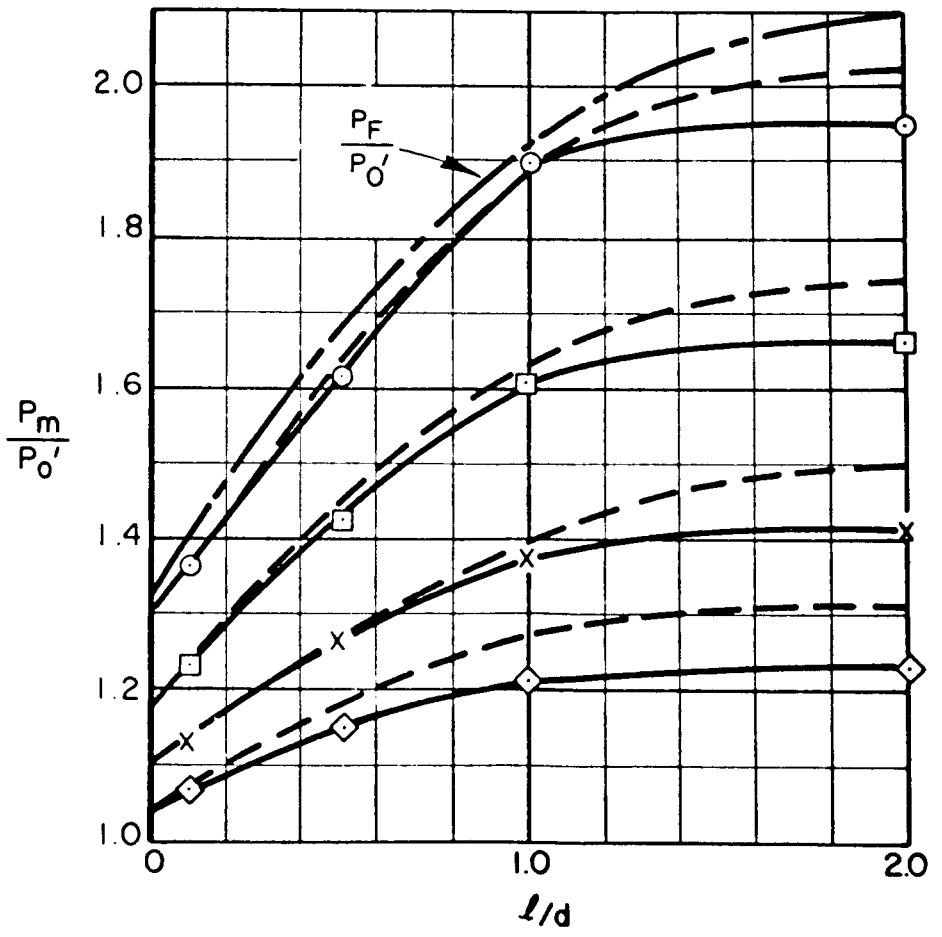

Figure 6b. Series B Impact Probe ℓ/d Effects, Mach No. 3.

SYMBOL	MACH NUMBER	Kn_D
⊙	5.46	2.33
⊡	6.19	0.94
◇	6.55	0.57
X	6.84	0.27

— — — —THEORY

$T_W = T_O$

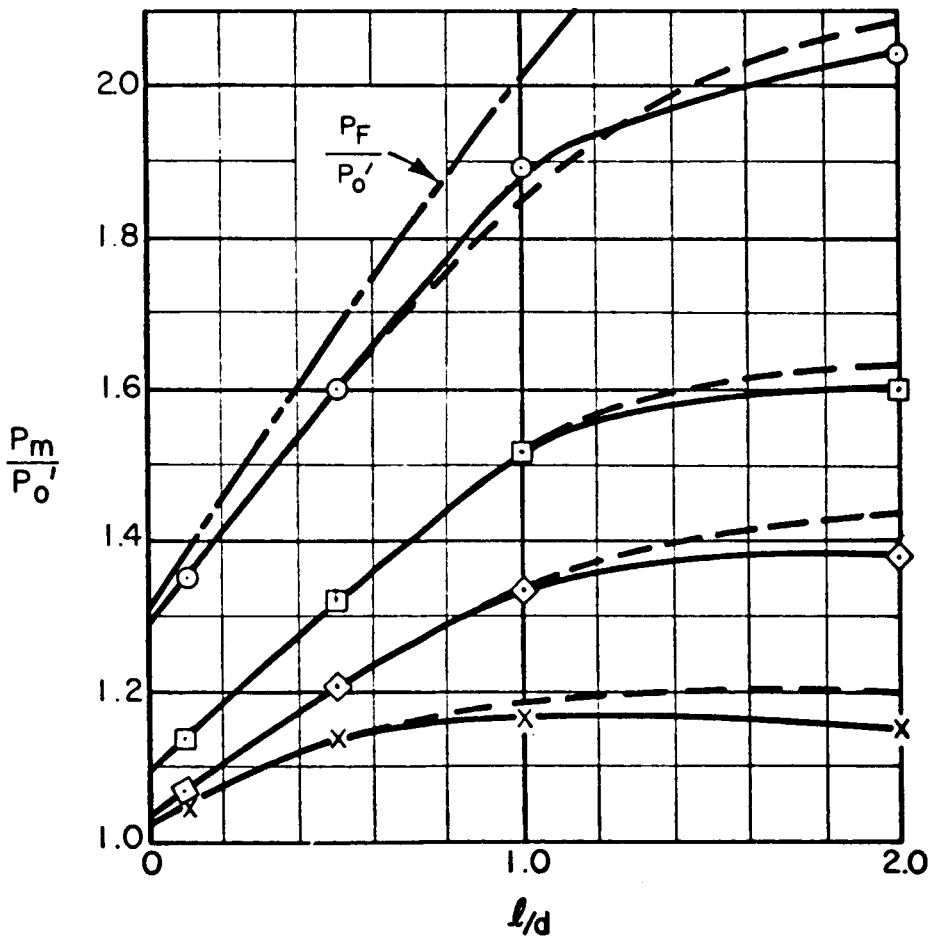

Figure 6c. Series B Impact Probe ℓ/d Effects, Mach No. 6.

SYMBOL	MACH NUMBER	Kn_D
⊙	9.77	.761
⊡	10.25	.665
◇	10.88	.439

$T_W = T_O$

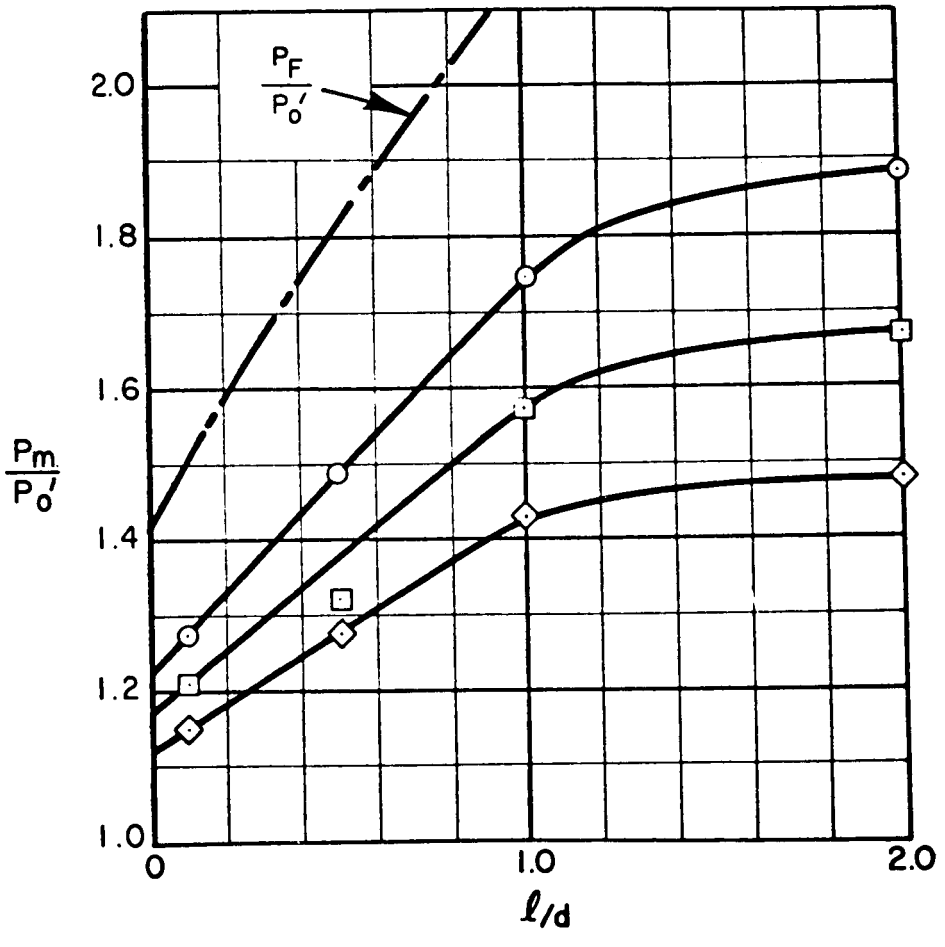

Figure 6d. Series B Impact Probe ℓ/d Effects, Mach No. 10.

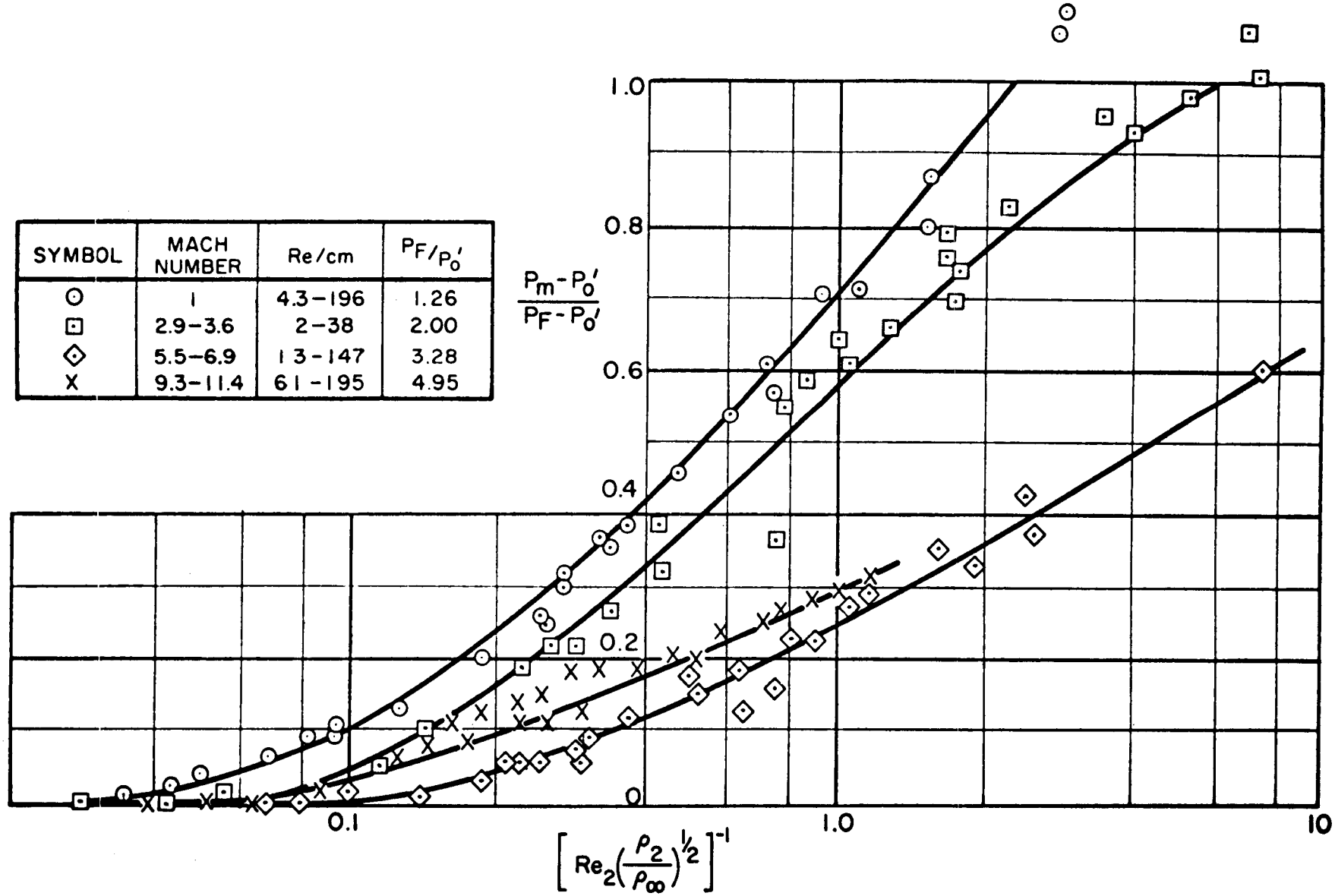

Figure 7. Series C Impact Probe Correlation, Mach Nos. 1, 3, 6 and 10.

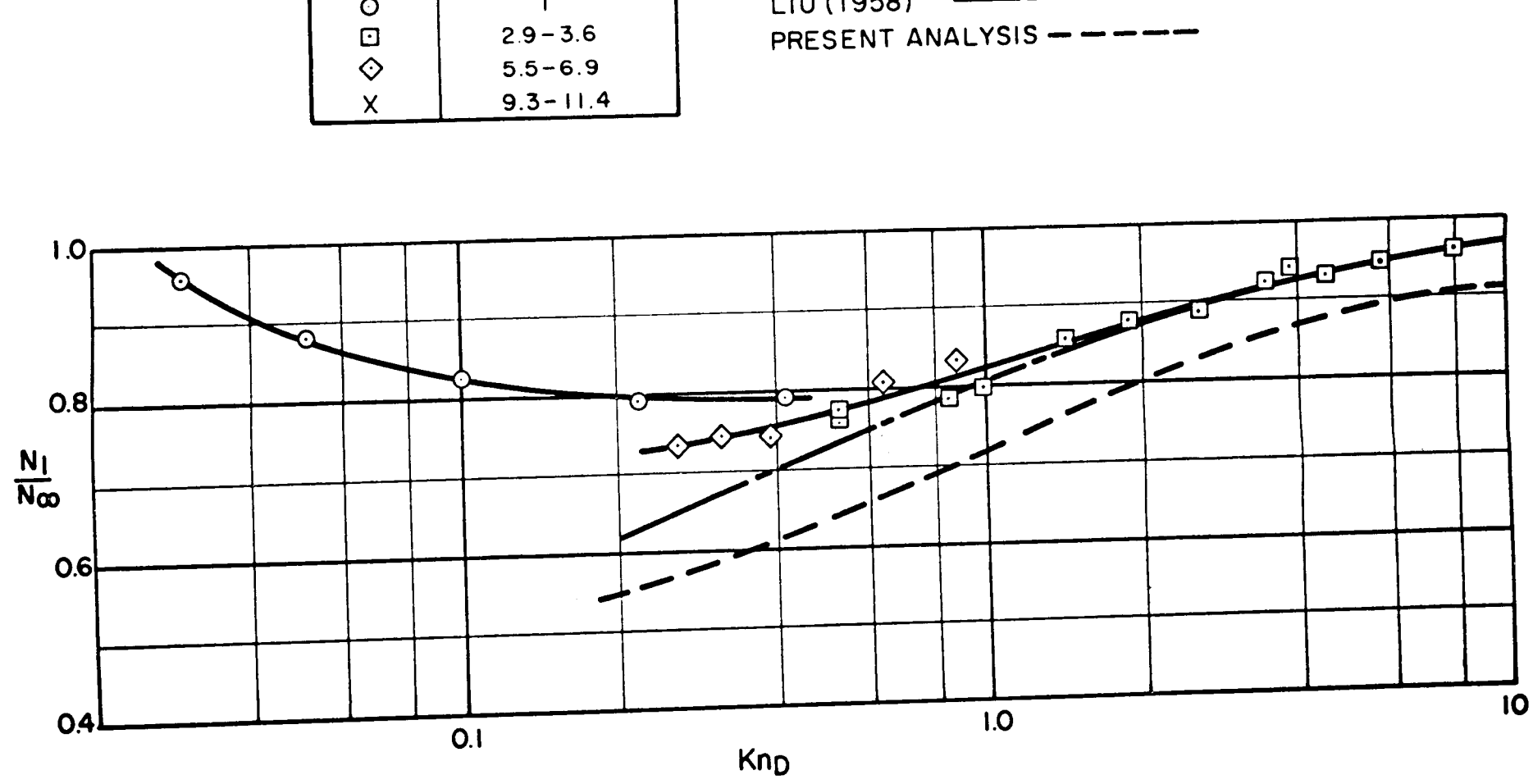

Figure 8 External Scattering Measurements.

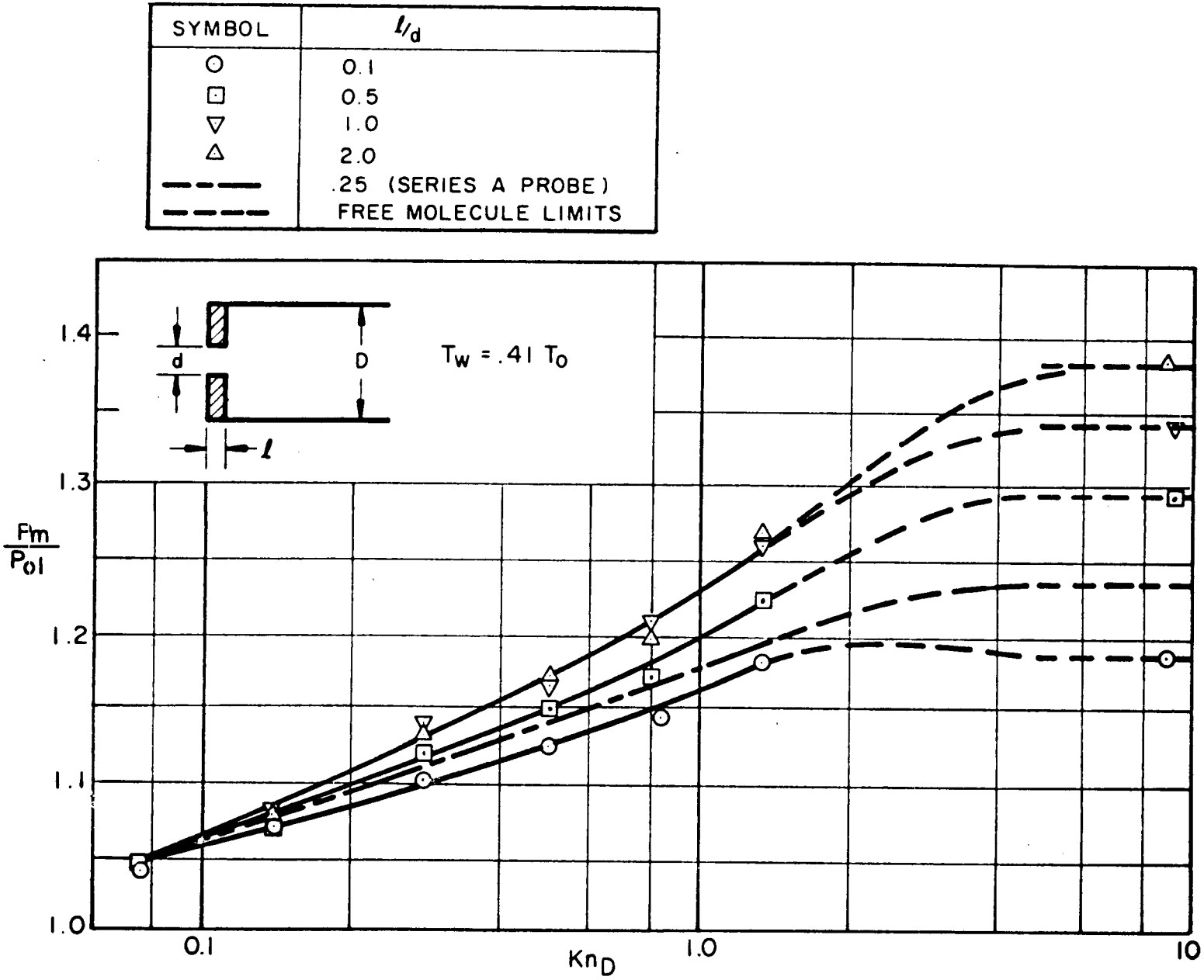

Figure 9a. Response of Series B Probes with Wall Cooling, Mach No. 1.

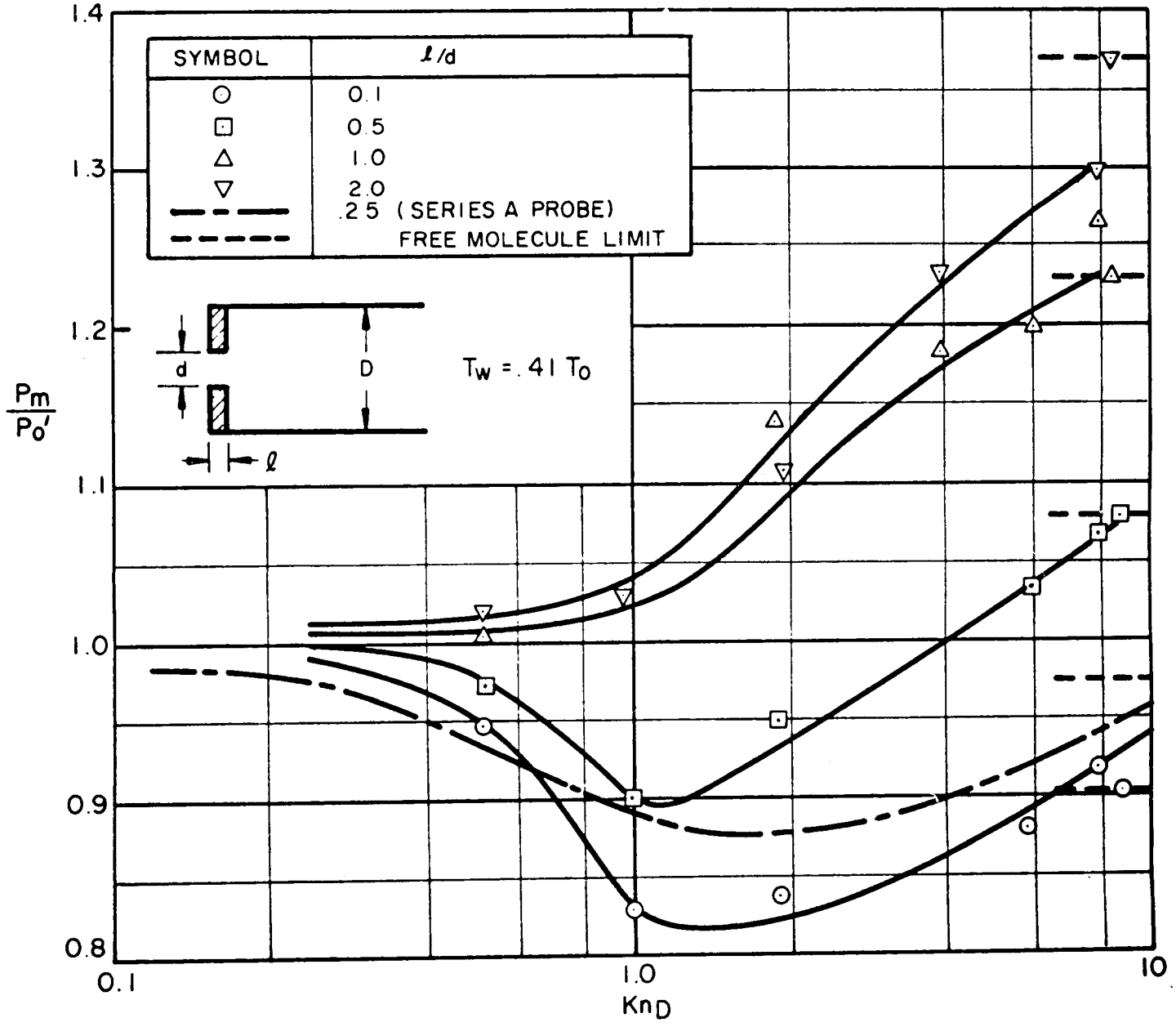

Figure 9b. Response of Series B Probes with Wall Cooling, Mach No. 3.

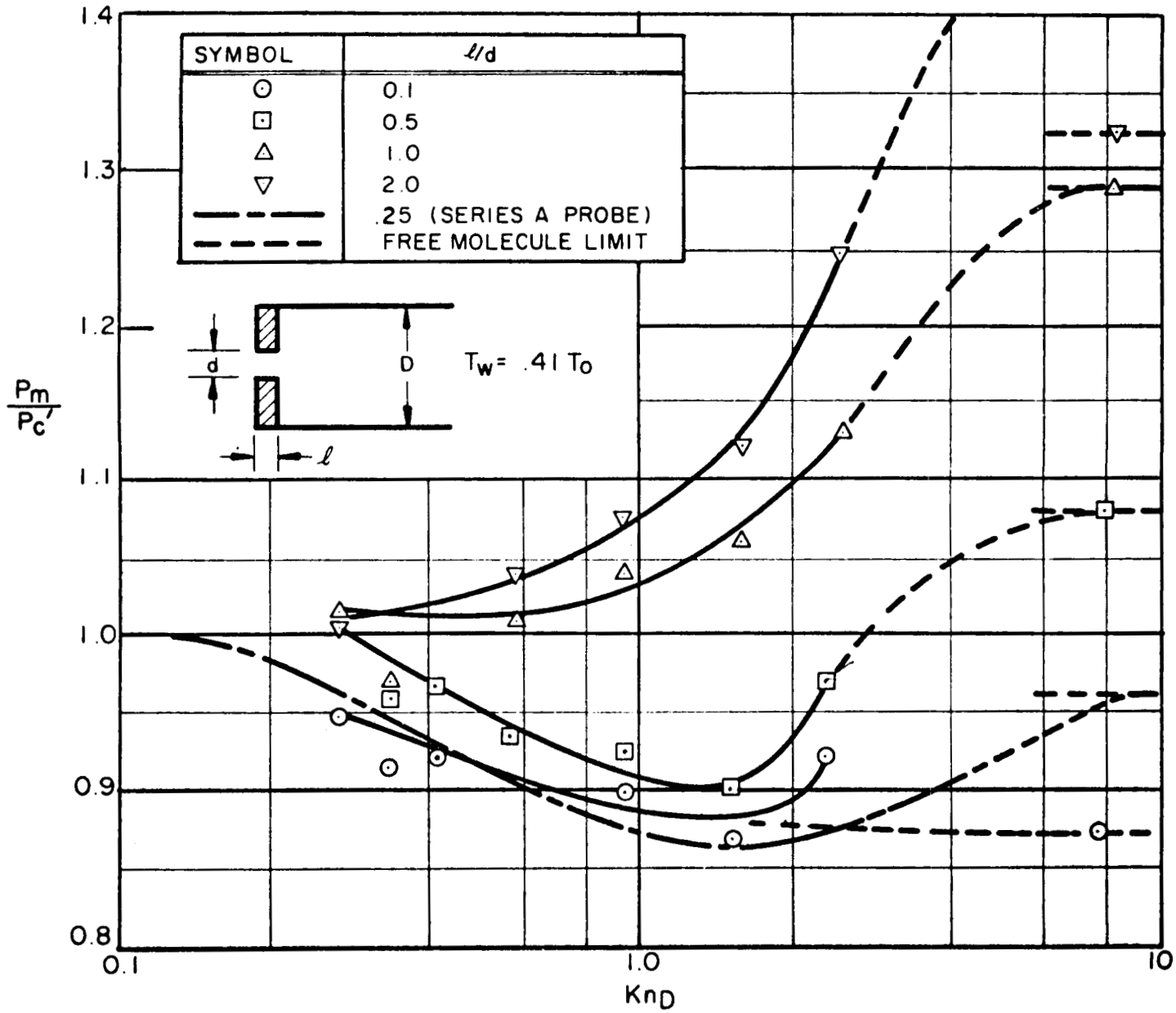

Figure 9c. Response of Series B Probes with Wall Cooling, Mach No. 6.

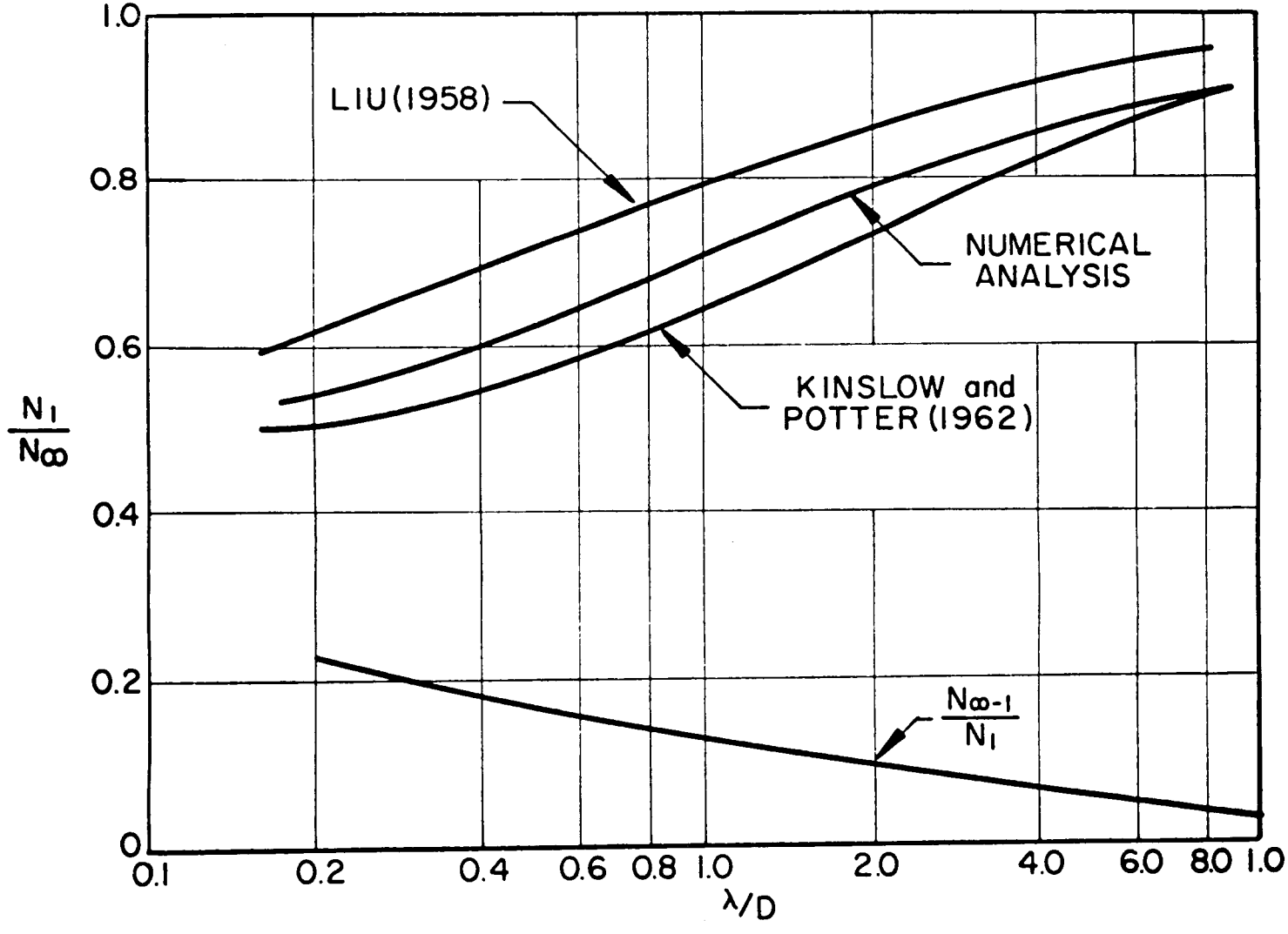

Figure 10. Variation of External and Internal Scattering with Knudsen Number.

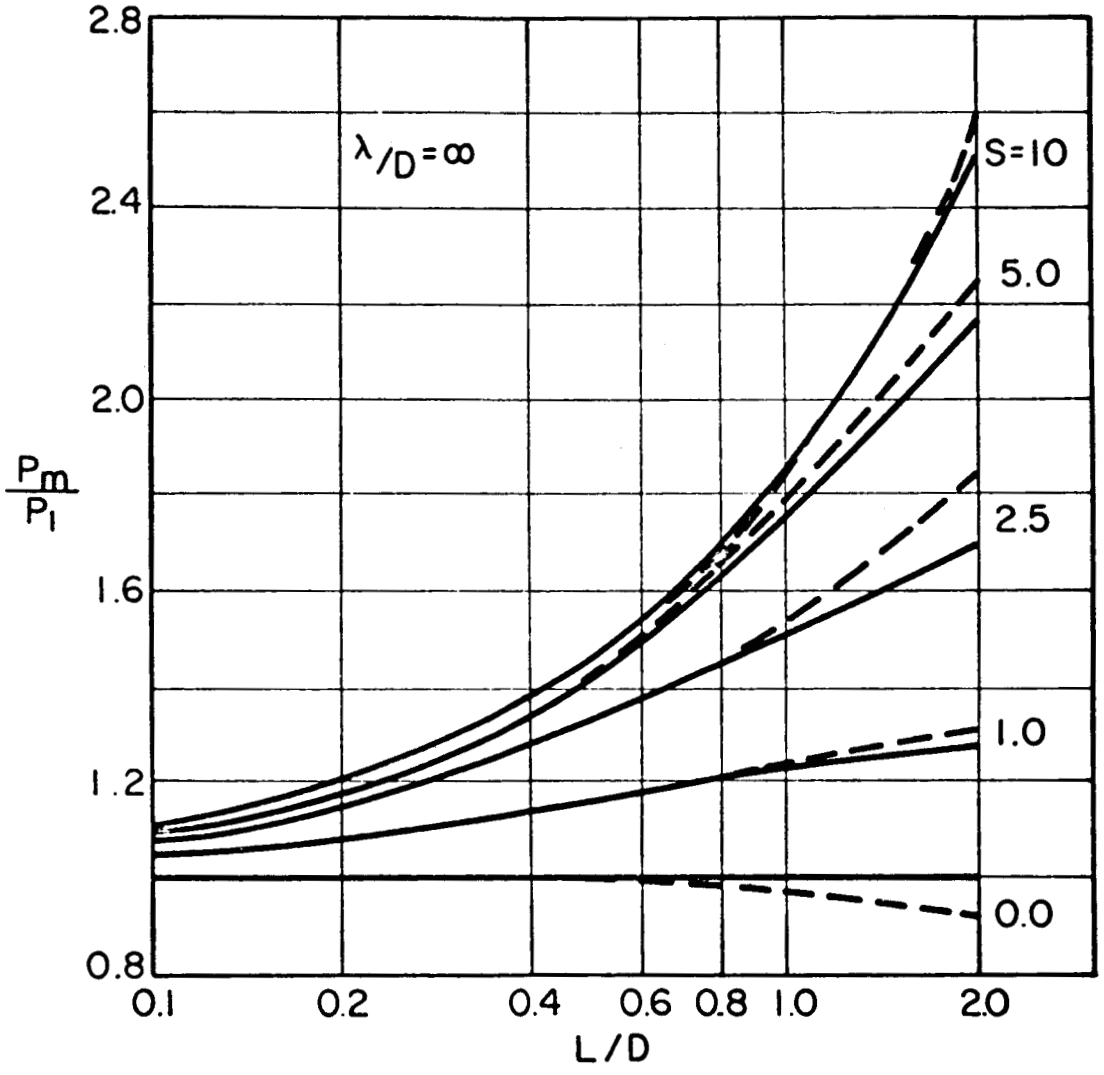

Figure 11a. Variation of Pressure Rise Across a Tube With L/D. Solid Curve: Numerical Approach of de Leeuw and Rothe (1962); Dashed Curve Eq. (17).

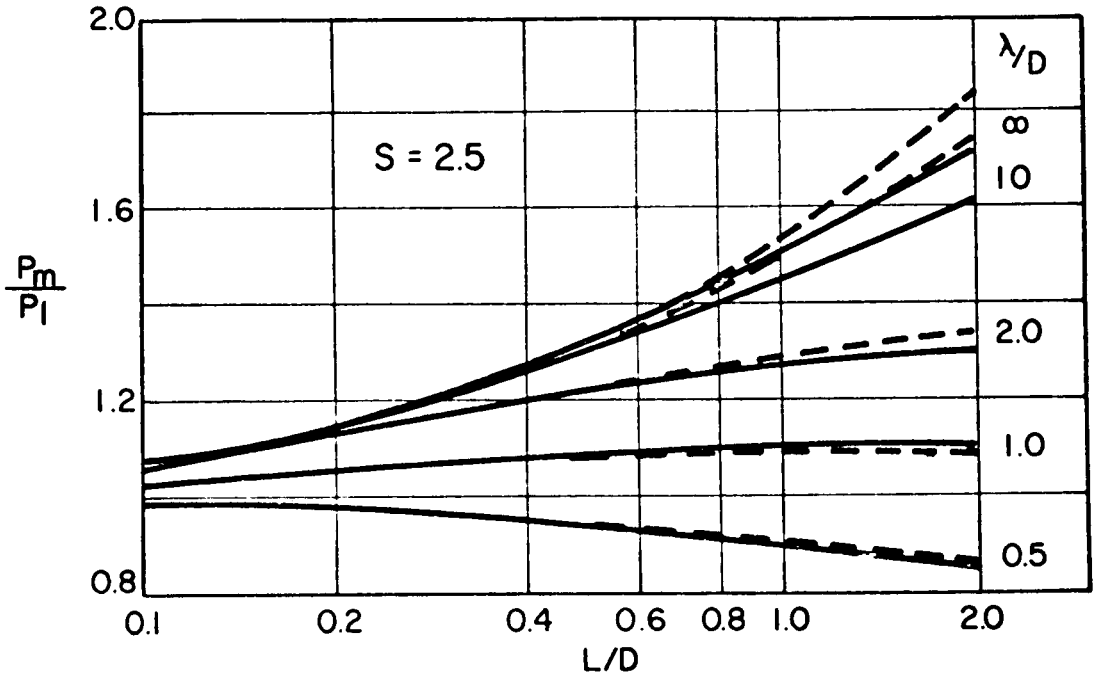

Figure 11b. Variation of Pressure Rise Across a Tube With L/D. Solid Curve: Numerical Approach of de Leeuw and Rothe (1962); Dashed Curve Eq. (17).

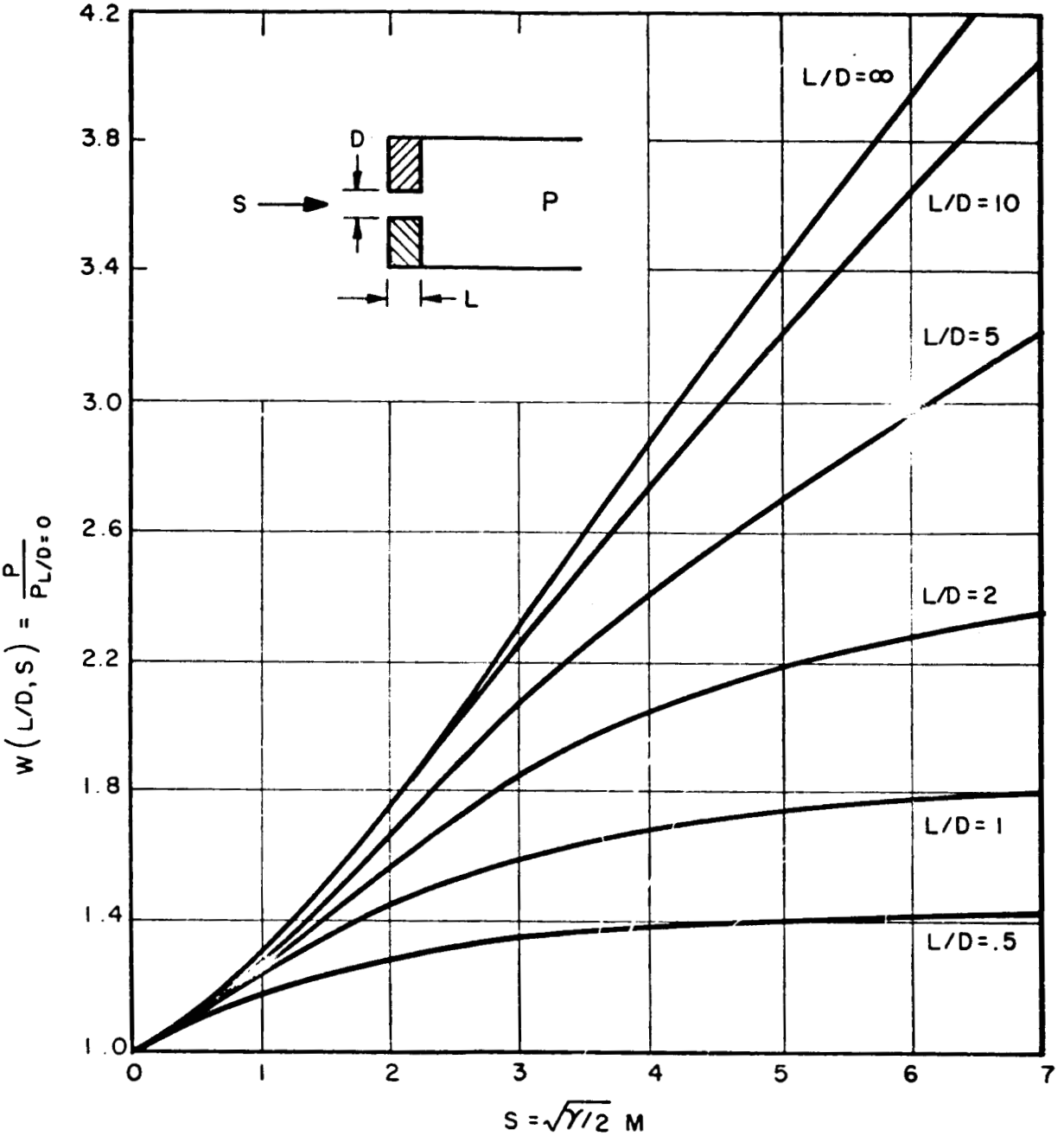

Figure 12. Free Molecule Impact Probe L/D Effects.

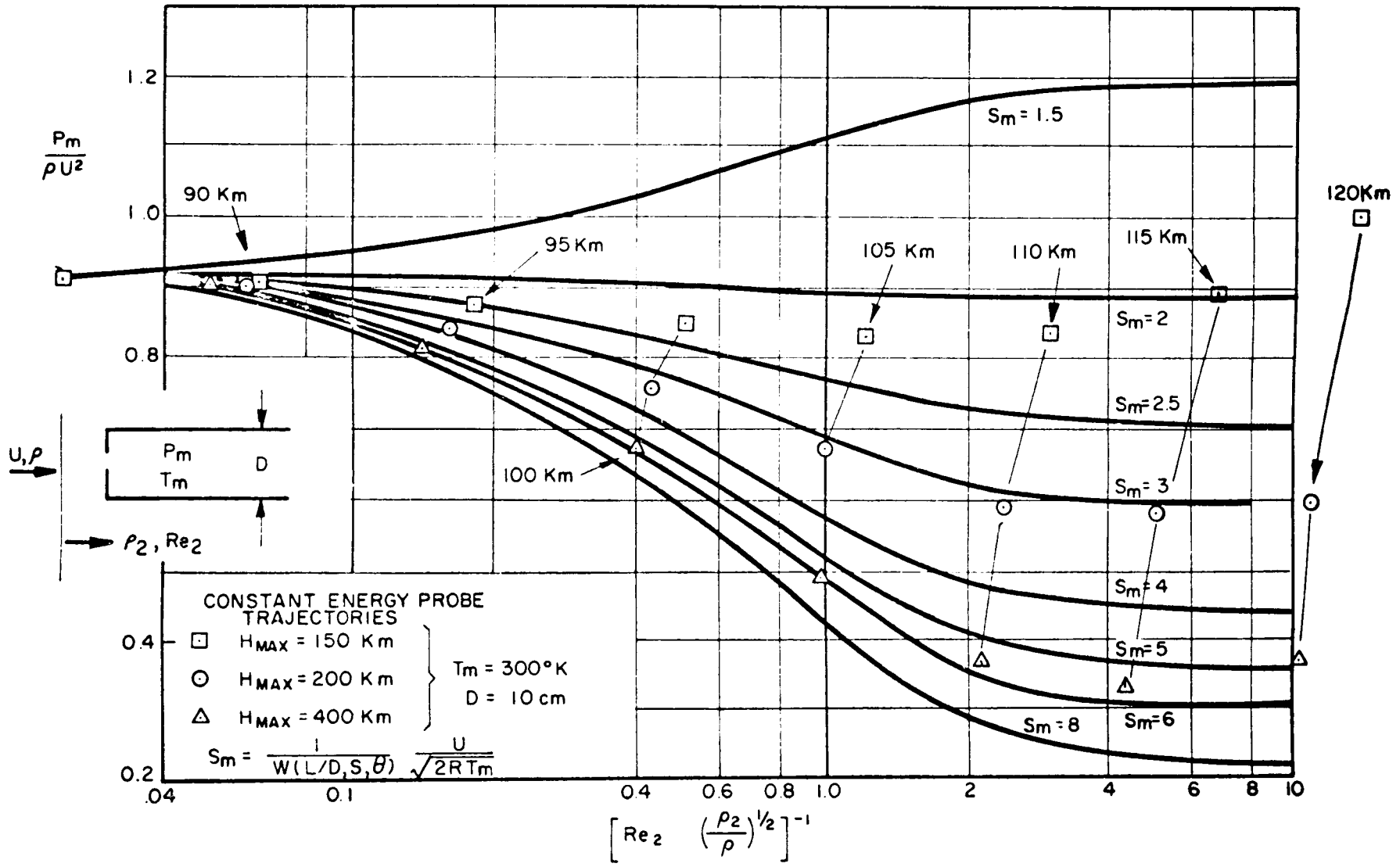

Figure 13. Impact Probe Response Characteristics.

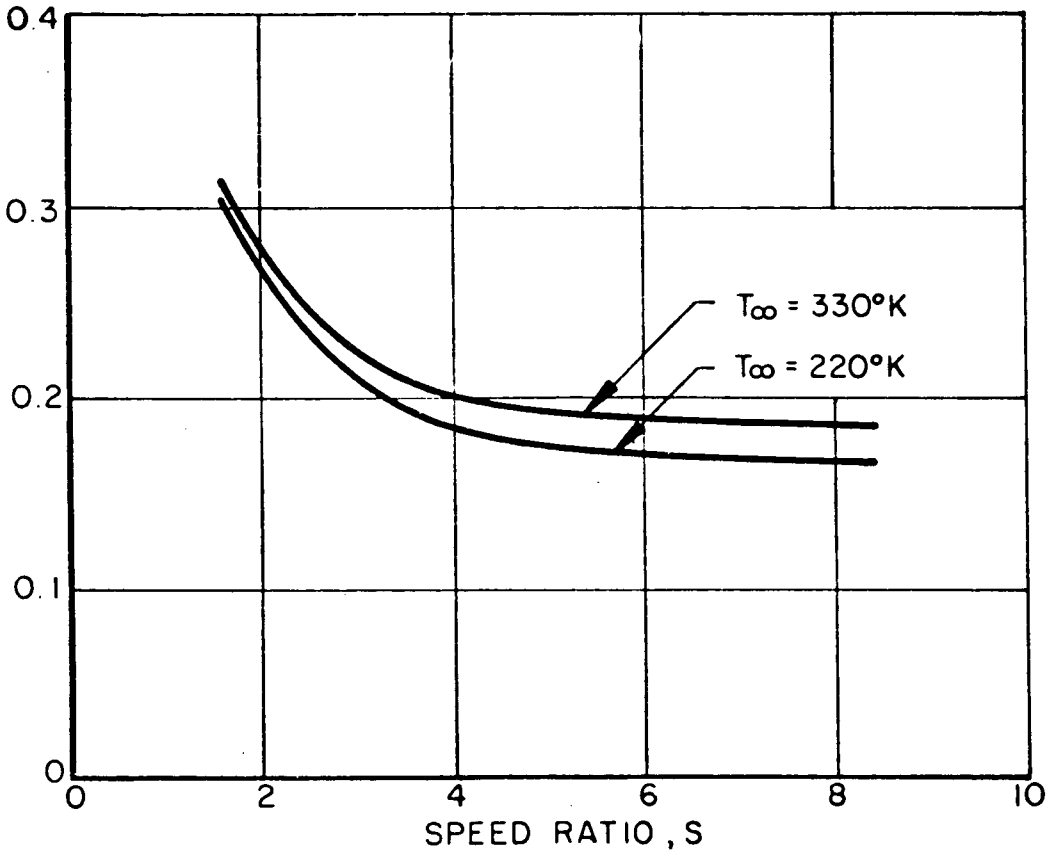

Figure 14. Variation of the Ratio

$$\left[Re_2 \left(\frac{\rho_2}{\rho_\infty}\right)^{\frac{1}{2}} \right]^{-1} \Big/ \lambda_{yD}$$

with Speed Ratio.

DISTRIBUTION

DIR

R-DIR

R-ASTR
Dr. Haeussermann

R-P&VE
Dr. Lucas
Mr. Riehl

R-RP
Dr. Stuhlinger
Mr. Heller
Dr. Shelton
Mr. Jones
Mr. Duncan

MS-IP

MS-IPL (8)

MS-T (5)

MS-H

HME-P

CC-P

R-AERO
Dr. Geissler
Mr. Vaughan
Mr. Scoggins
Mr. Dahm
Dr. Speer
Mr. Horn
Mr. Ballance (20)
Mr. Carter

EXTERNAL

Scientific & Technical Information Facility
P. O. Box 33
College Park, Maryland (25)
Attn: NASA Representative (S-AK/RKT)

Langley Research Center
Langley Station
Hampton, Virginia

Oak Ridge National Laboratory
Oak Ridge, Tenn.

University of Minnesota
Minneapolis, Minn.

Dr. Robert Young
University of Tennessee Research Inst.
AEDC
Tullahoma, Tenn.

Mason Charak
Code RV-1
NASA Headquarters
Washington, D. C.

Lewis Research Center
21000 Brookpark
Cleveland, Ohio
Attn: Dr. Herman Mark
Mr. Lloyd Krause
Mr. Edward Richley
Library

Goddard Space Flight Center
Greenbelt, Md.
Attn: Mr. George Newton
Library

Heat Technology Laboratory
Huntsville, Alabama
S. J. Robertson

DISTRIBUTION (concluded)

JPL
4800 Oak Grove Dr.
Pasadena, Calif.

Ames Research Center
Moffett Field, Calif.

Manned Spacecraft Center
Houston, Texas
Attn: William K. Roberts
Library

Arthur D. Little, Inc.
Cambridge, Mass.
Attn: Raymond Moore

Northrop Space Laboratories
Huntsville, Ala.
Attn: T. M. McCoy

AEDC
Arnold Air Force Station, Tenn.
Attn: Lt. Col. John Peters
Capt. George Mushalko

ARO, Inc.
AEDC
Arnold Air Force Station, Tenn.
Attn: Mr. George Kirby
E. K. Latvala
Library

University of Illinois
Urbana, Ill.

Dr. Robert Stickney
Rm. 3-350
MIT
Cambridge, Mass.

Dr. A. B. Huang
Georgia Institute of Technology
Atlanta, Ga.

Celestrial Research Corporation
1015 Fremont Ave.
South Pasadena, Calif
Attn: Dr. Raymond Chuan
Mr. John Wainwright (20)
Mr. Don Wallace

University of Alabama
University, Alabama
Attn: Dr. Walter Schaetzle

Institute of Aerophysics
University of Toronto
Toronto, Canada

Cornell Aeronautical Lab., Inc.
Buffalo, New York

McDonnell Aircraft Corp.
P. O. Box 516
St. Louis, Missouri
Attn: E. S. J. Wang

University of Calif. Radiation Lab.
Livermore, Calif.

Lockheed Aircraft Corp.
Huntsville, Ala.
Attn: Mr. M. Culp
Mr. T. Cunningham
Mr. L. Morrison
Library

Brown Engineering Co.
Huntsville, Ala.
Attn: Mr. D. Tarbell
Library

University of Michigan
Ann Arbor, Michigan
Attn: Dr. A. G. Hansen
Library